FIG. 1

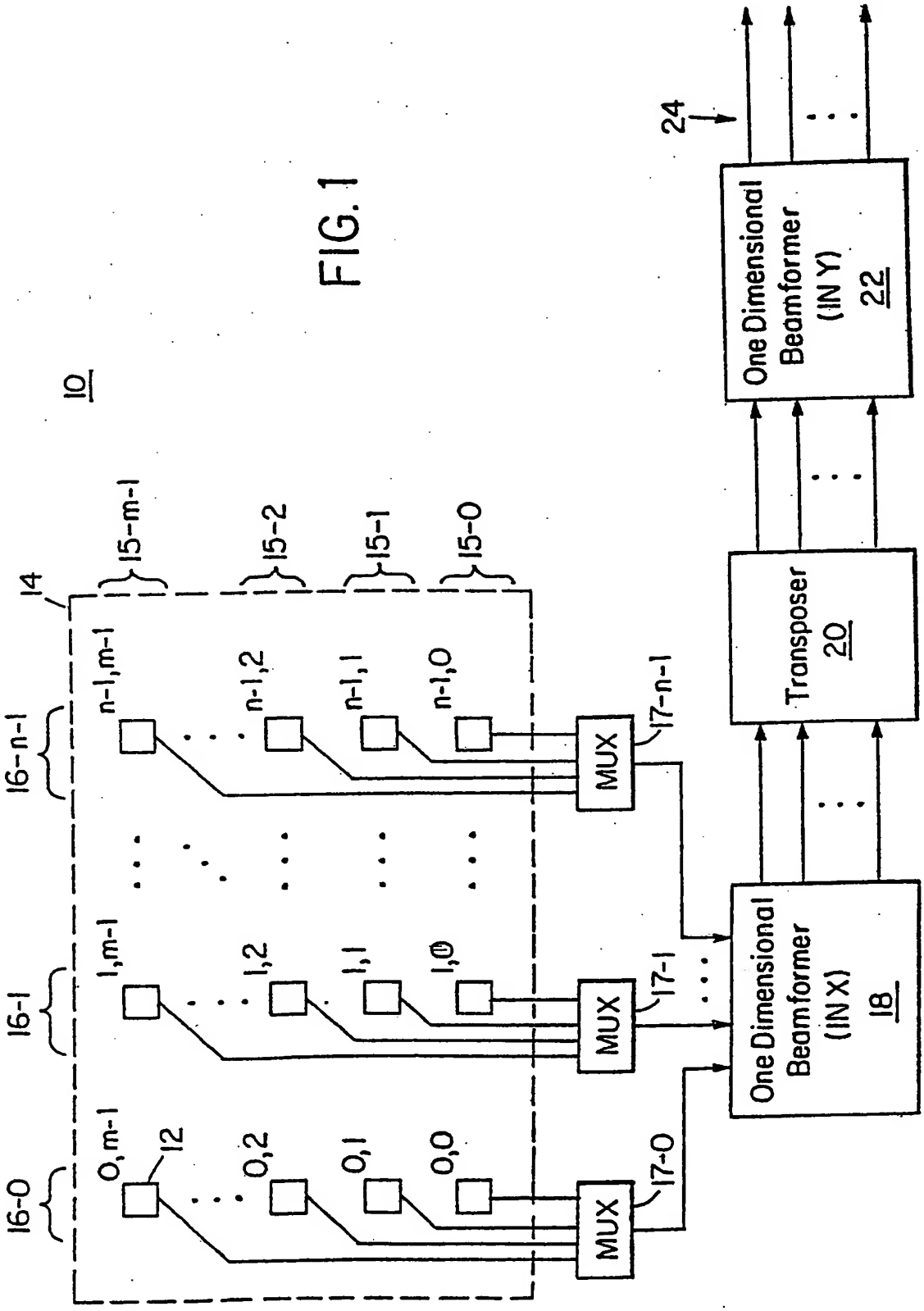
10
14
15-m-1
15-2
15-1
15-0
16-n-1
16-1
16-0
n-1,m-1
n-1,2
n-1,1
n-1,0
1,m-1
1,2
1,1
1,0
0,m-1
12
0,2
0,1
0,0
MUX
MUX
MUX
17-n-1
17-1
17-0
24
One Dimensional Beamformer (IN Y) 22
Transposer 20
One Dimensional Beamformer (IN X) 18

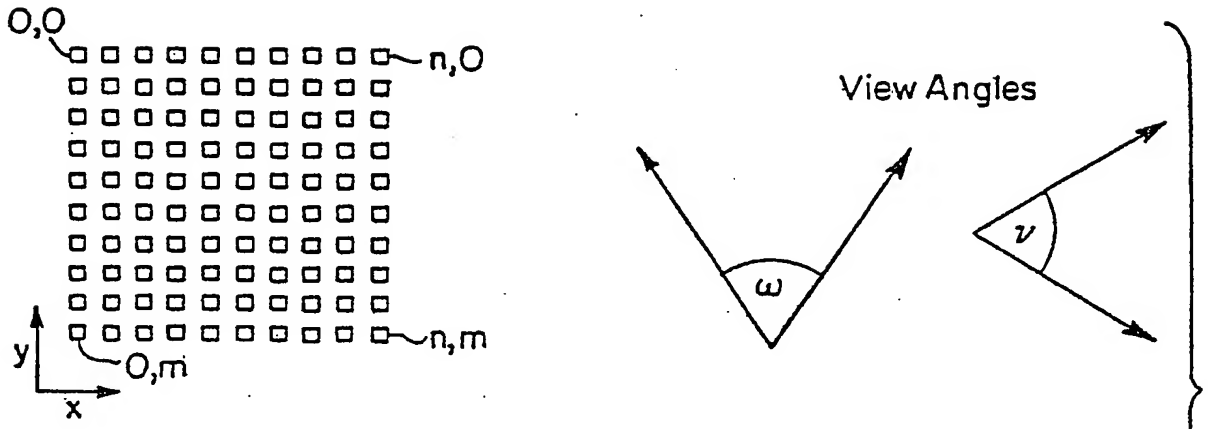

$D_{x,y}$ —Input in from sensor col x, row y

$D_{x,\nu}$ —Inputs from col x beam-formed at angle ν

$D_{\omega,y}$ —Inputs from row y beam-formed at angle ω

$D_{\omega,\nu}$ —Inputs beam-formed at angles ω,ν

$D_{\omega,\nu}[t]$—Inputs beam-formed at angles ω,ν at time (depth) t

FIG. 2

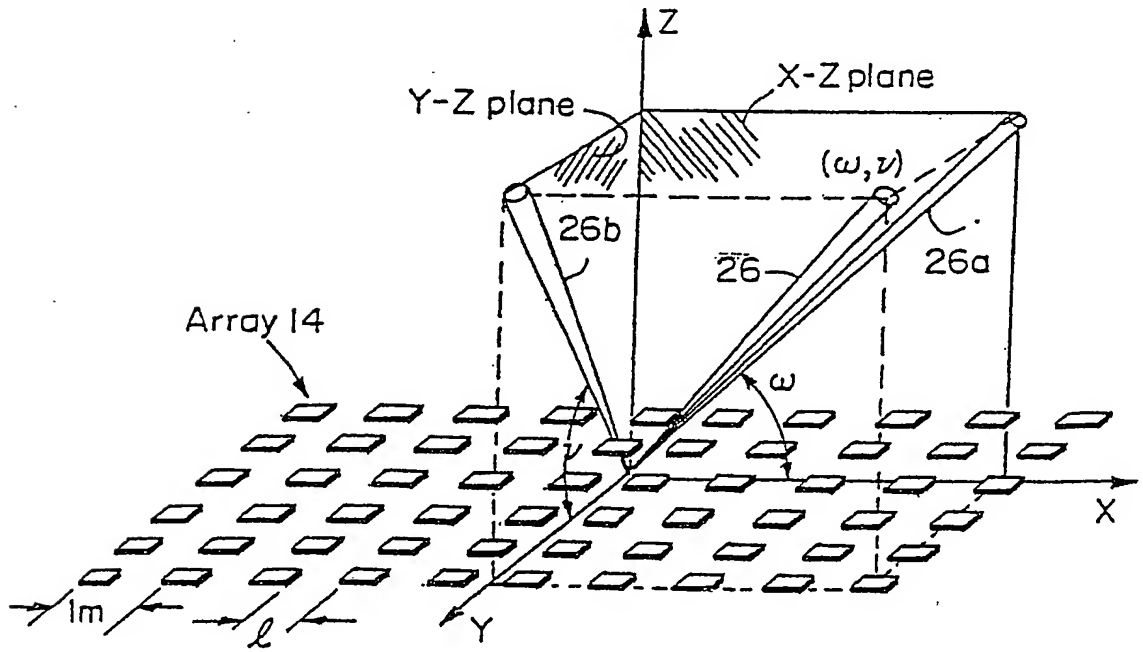

FIG. 3

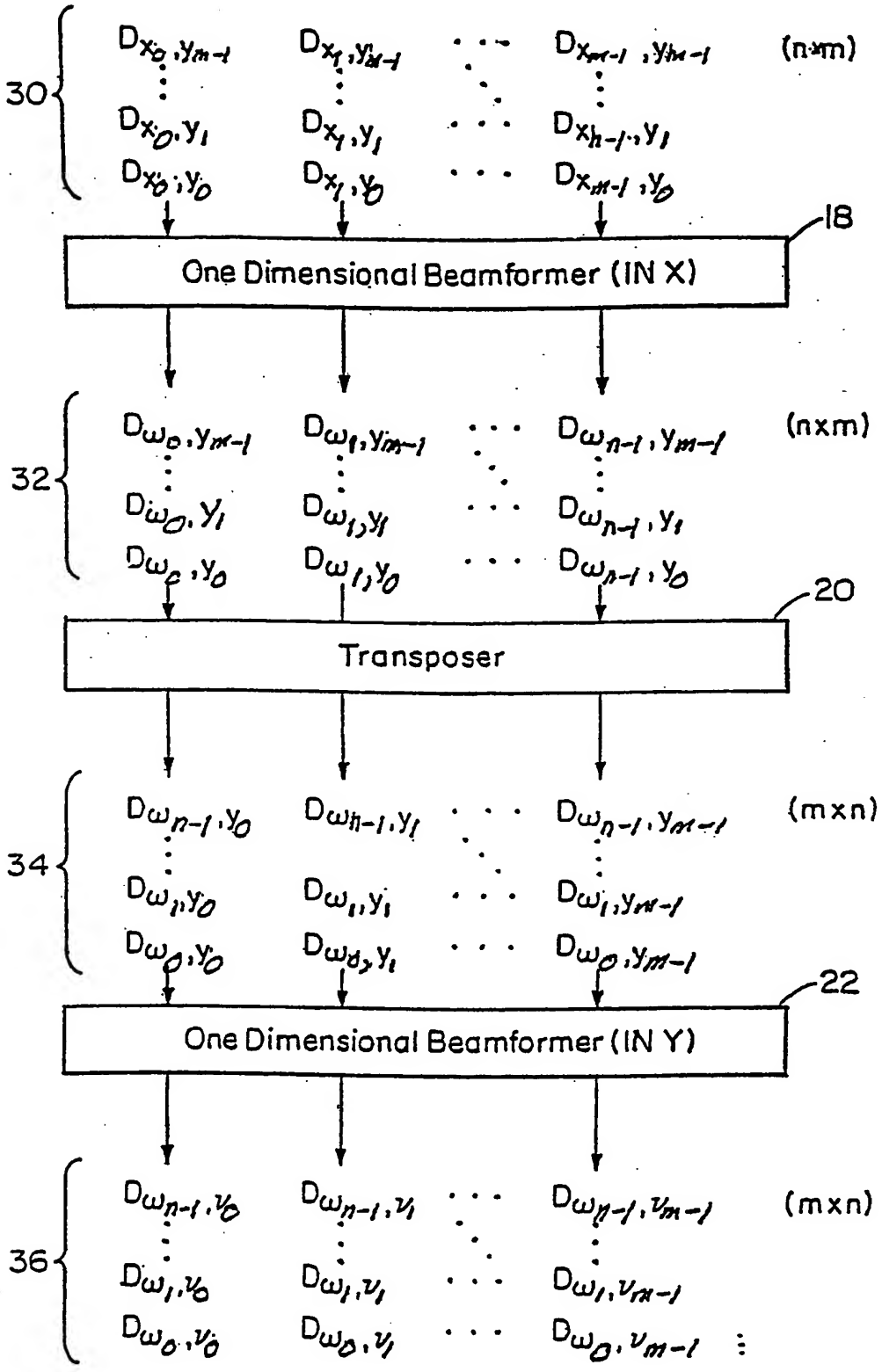
30
(n×m)
18
One Dimensional Beamformer (IN X)
32
(n×m)
20
Transposer
34
(m×n)
22
One Dimensional Beamformer (IN Y)
36
(m×n)

FIG. 4

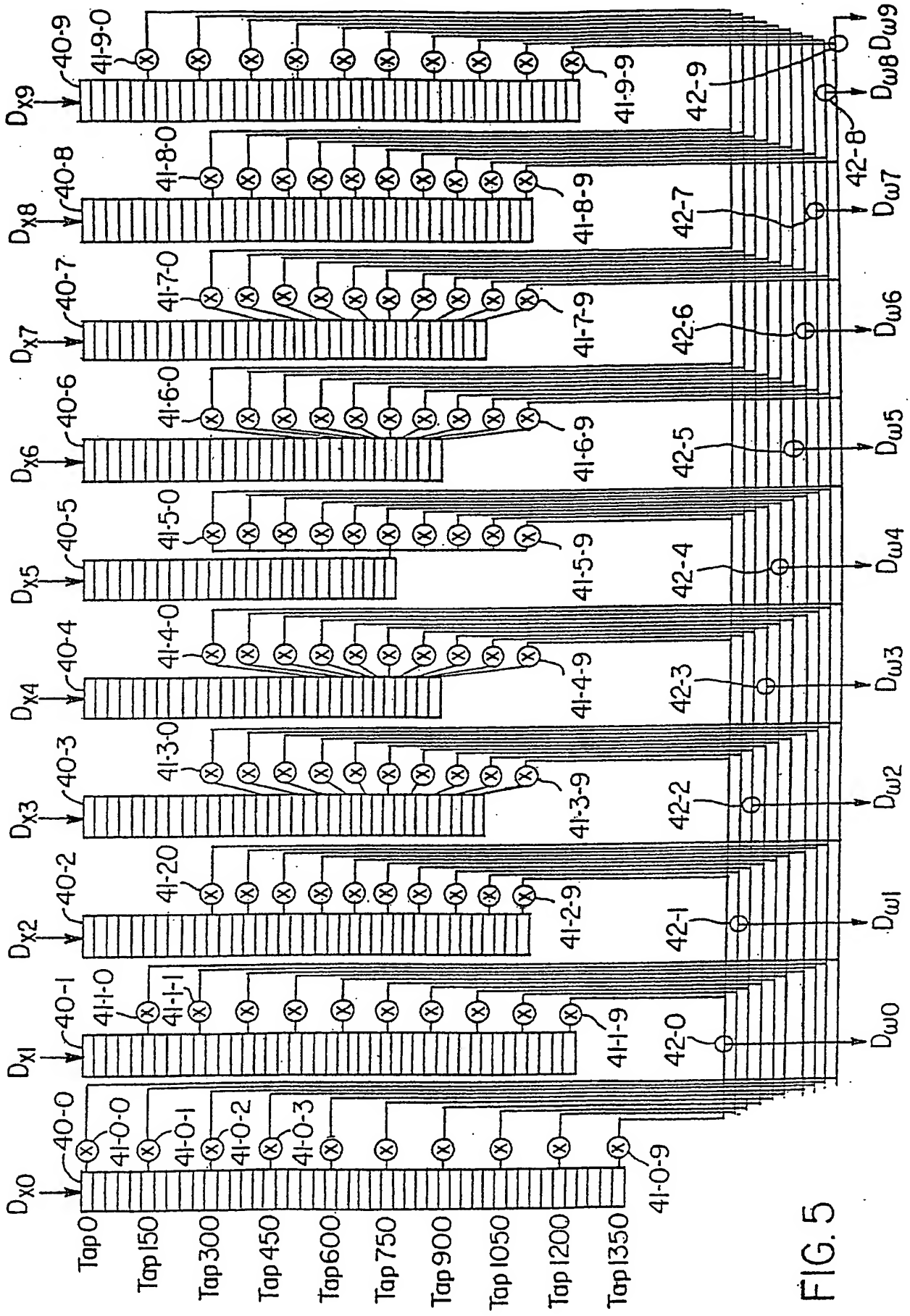
Dx0
Dx1
Dx2
Dx3
Dx4
Dx5
Dx6
Dx7
Dx8
Dx9
40-0
40-1
40-2
40-3
40-4
40-5
40-6
40-7
40-8
40-9
41-0-0
41-0-1
41-0-2
41-0-3
41-0-9
41-1-0
41-1-1
41-1-9
41-20
41-2-9
41-3-0
41-3-9
41-4-0
41-4-9
41-5-0
41-5-9
41-6-0
41-6-9
41-7-0
41-7-9
41-8-0
41-8-9
41-9-0
41-9-9
42-0
42-1
42-2
42-3
42-4
42-5
42-6
42-7
42-8
42-9
Dω0
Dω1
Dω2
Dω3
Dω4
Dω5
Dω6
Dω7
Dω8
Dω9
Tap 0
Tap 150
Tap 300
Tap 450
Tap 600
Tap 750
Tap 900
Tap 1050
Tap 1200
Tap 1350

FIG. 5

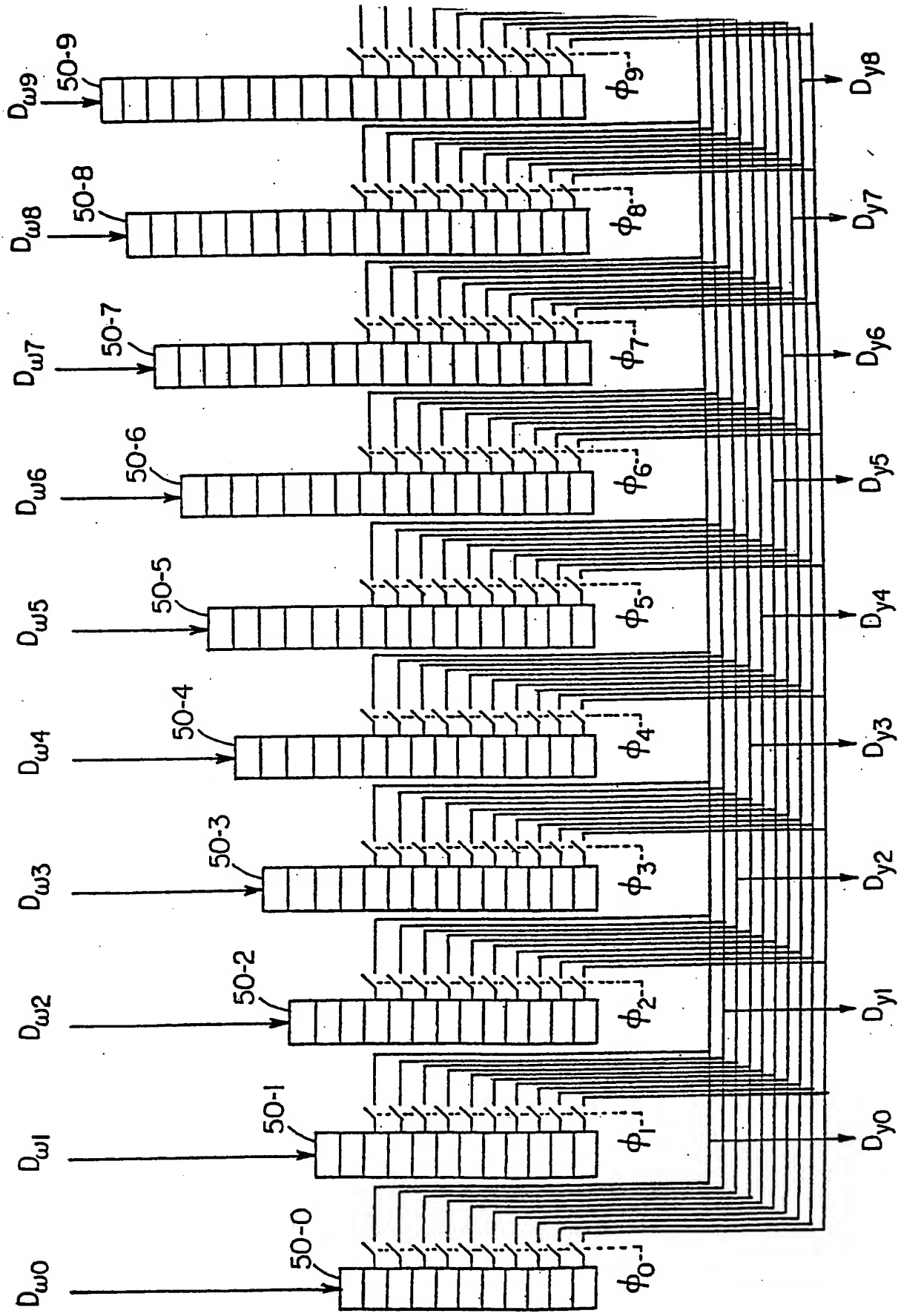
$D_{\omega 9}$
50-9
ϕ_{9-j}
D_{y8}
$D_{\omega 8}$
50-8
ϕ_{8-j}
D_{y7}
$D_{\omega 7}$
50-7
ϕ_{7-j}
D_{y6}
$D_{\omega 6}$
50-6
ϕ_{6-j}
D_{y5}
$D_{\omega 5}$
50-5
ϕ_{5-j}
D_{y4}
$D_{\omega 4}$
50-4
ϕ_{4-j}
D_{y3}
$D_{\omega 3}$
50-3
ϕ_{3-j}
D_{y2}
$D_{\omega 2}$
50-2
ϕ_{2-j}
D_{y1}
$D_{\omega 1}$
50-1
ϕ_{1-j}
D_{y0}
$D_{\omega 0}$
50-0
ϕ_{0-j}

FIG. 6

FIG. 7

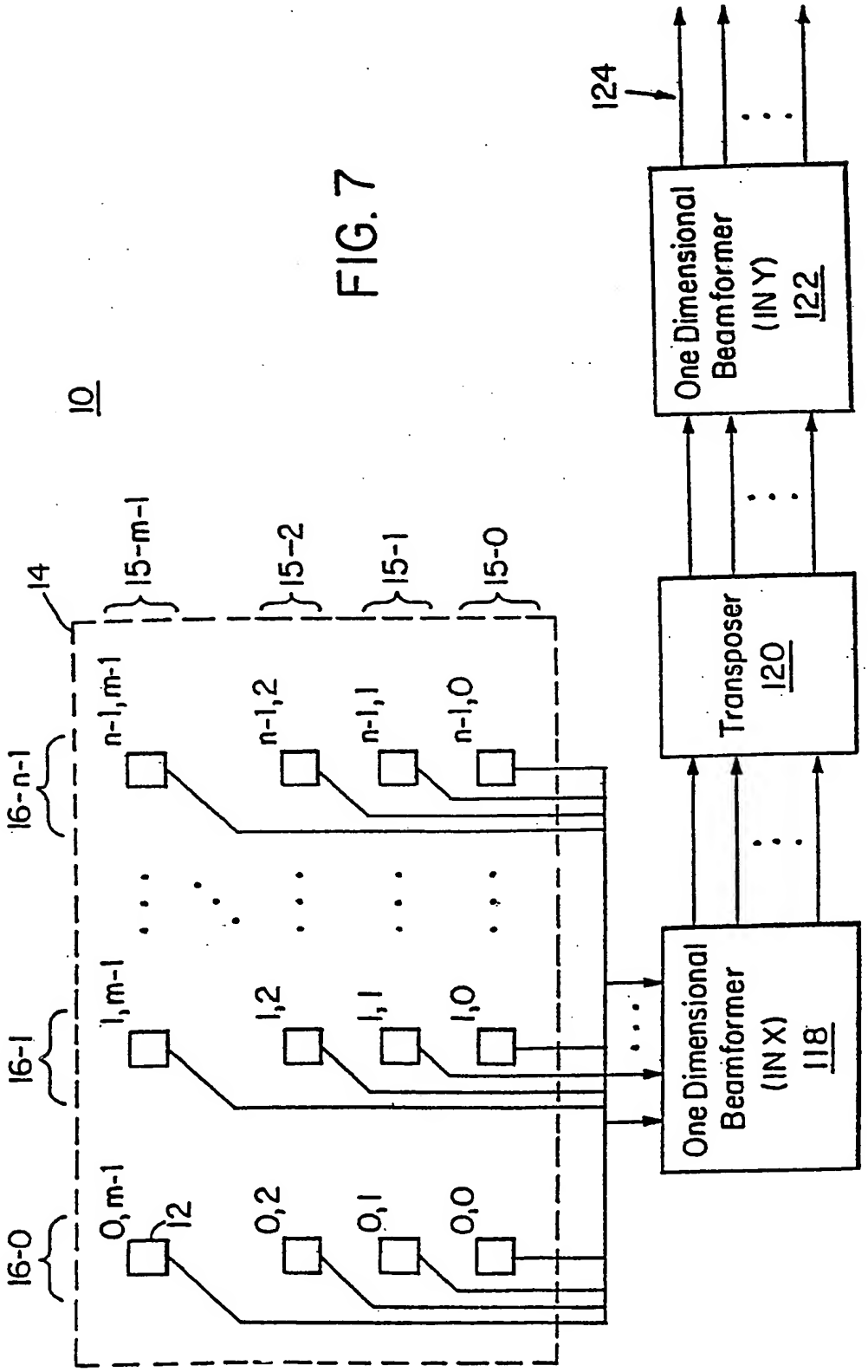
10
14
15-m-1
15-2
15-1
15-0
16-n-1
16-1
16-0
n-1,m-1
n-1,2
n-1,1
n-1,0
1,m-1
1,2
1,1
1,0
0,m-1
0,2
0,1
0,0
12
One Dimensional Beamformer (IN X) 118
Transposer 120
One Dimensional Beamformer (IN Y) 122
124

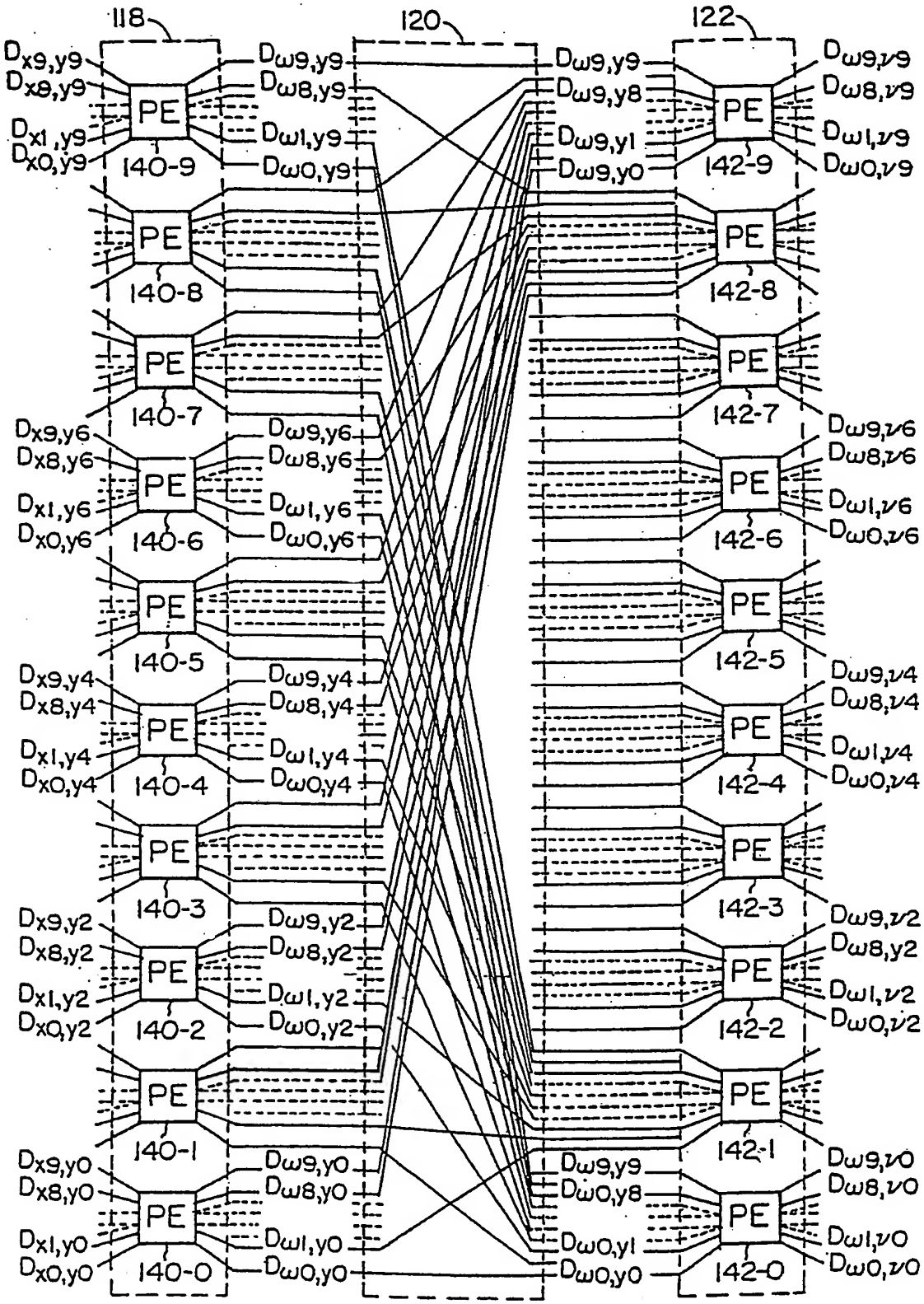
118
120
122
PE
140-9
140-8
140-7
140-6
140-5
140-4
140-3
140-2
140-1
140-0
142-9
142-8
142-7
142-6
142-5
142-4
142-3
142-2
142-1
142-0

FIG. 8

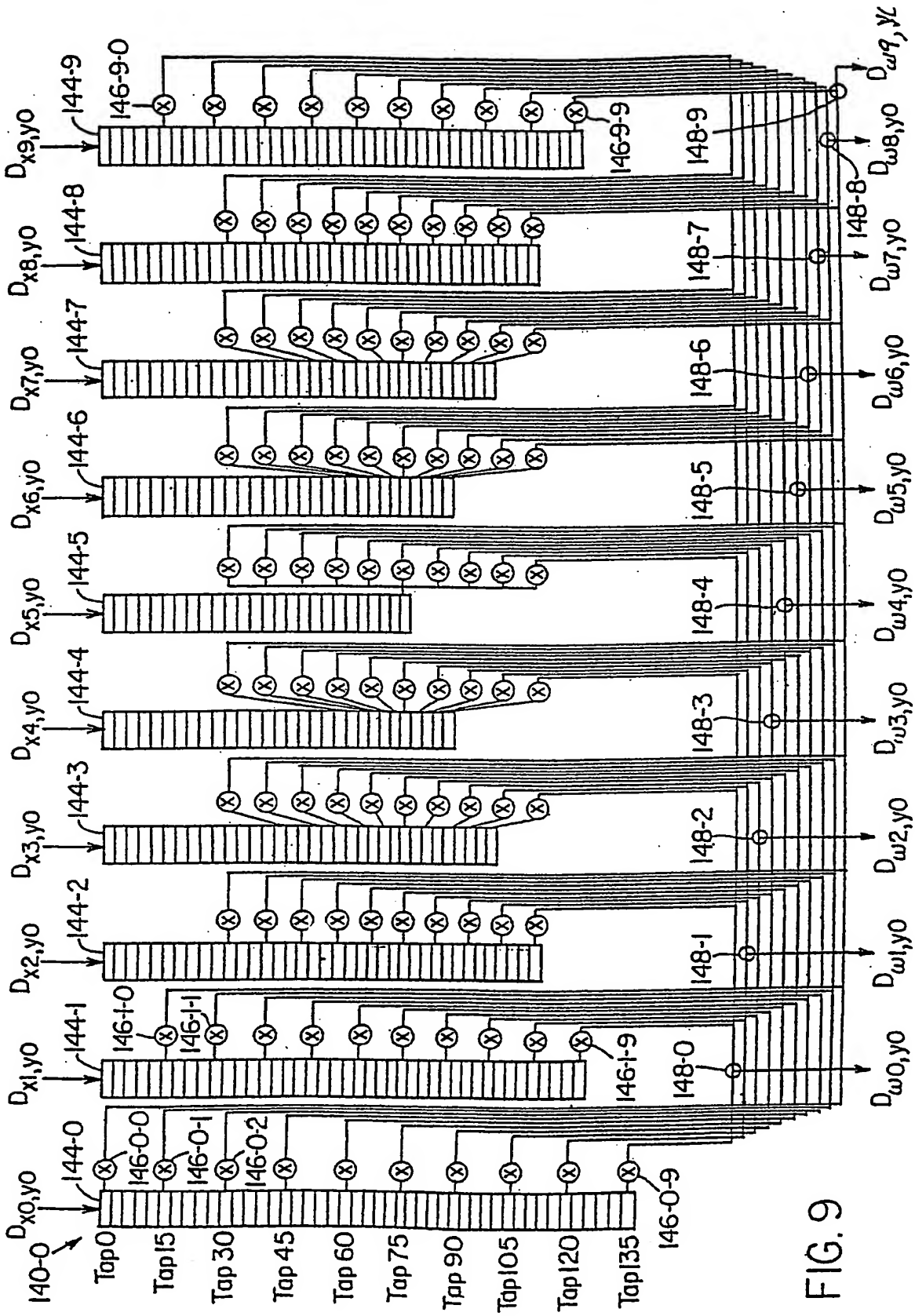
140-0
Tap0
Tap15
Tap30
Tap45
Tap60
Tap75
Tap90
Tap105
Tap120
Tap135
$D_{x0,y0}$
144-0
146-0-0
146-0-1
146-0-2
146-0-9
$D_{x1,y0}$
144-1
146-1-0
146-1-1
146-1-9
148-0
$D_{\omega 0,y0}$
$D_{x2,y0}$
144-2
148-1
$D_{\omega 1,y0}$
$D_{x3,y0}$
144-3
148-2
$D_{\omega 2,y0}$
$D_{x4,y0}$
144-4
148-3
$D_{\omega 3,y0}$
$D_{x5,y0}$
144-5
148-4
$D_{\omega 4,y0}$
$D_{x6,y0}$
144-6
148-5
$D_{\omega 5,y0}$
$D_{x7,y0}$
144-7
148-6
$D_{\omega 6,y0}$
$D_{x8,y0}$
144-8
148-7
$D_{\omega 7,y0}$
$D_{x9,y0}$
144-9
146-9-0
146-9-9
148-9
148-8
$D_{\omega 8,y0}$
$D_{\omega 9,y0}$

FIG. 9

FIG. 10

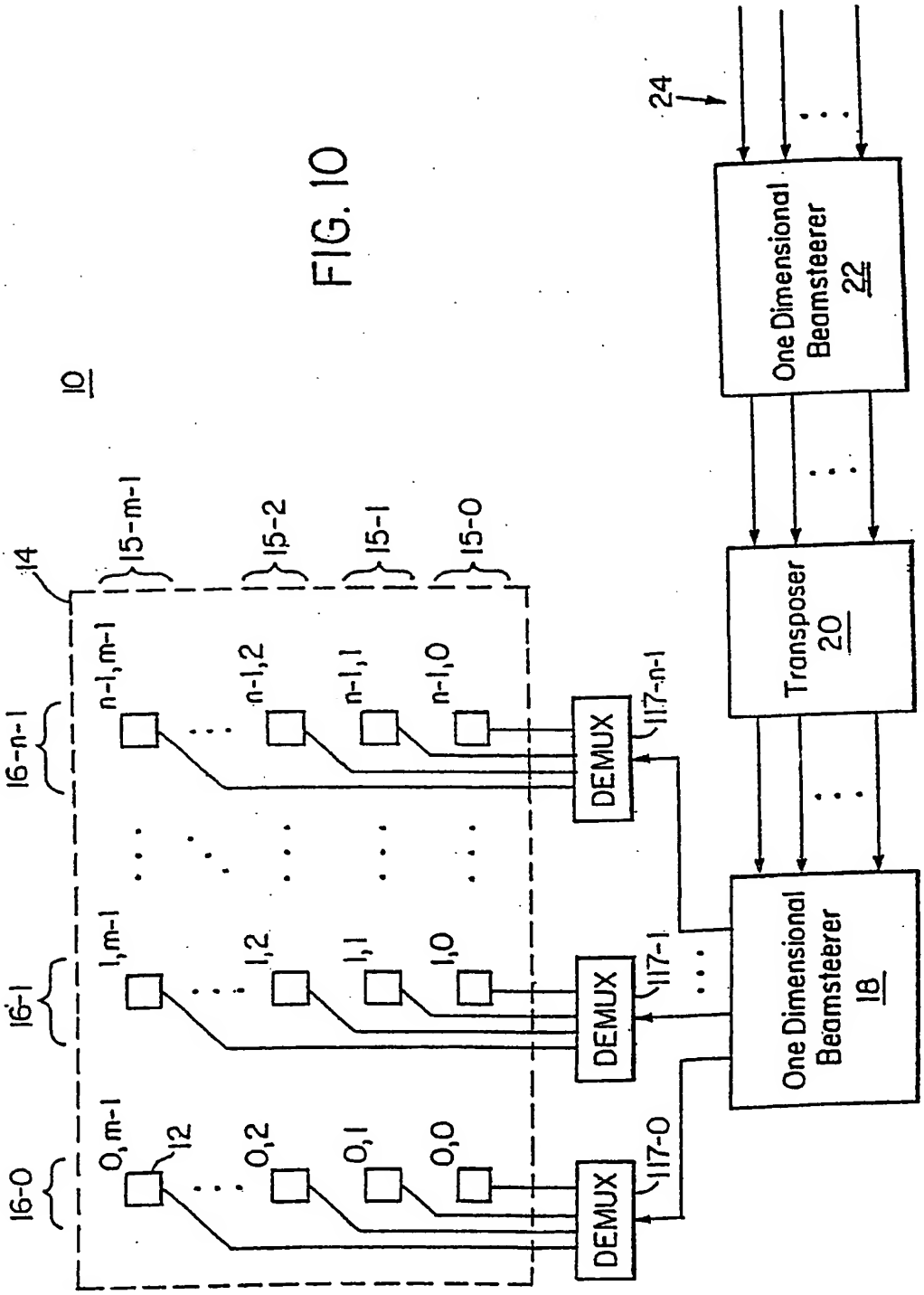
10
14
15-m-1
15-2
15-1
15-0
16-n-1
16-1
16-0
n-1,m-1
n-1,2
n-1,1
n-1,0
1,m-1
1,2
1,1
1,0
0,m-1
0,2
0,1
0,0
12
DEMUX
DEMUX
DEMUX
117-n-1
117-1
117-0
24
One Dimensional Beamsteerer 22
Transposer 20
One Dimensional Beamsteerer 18

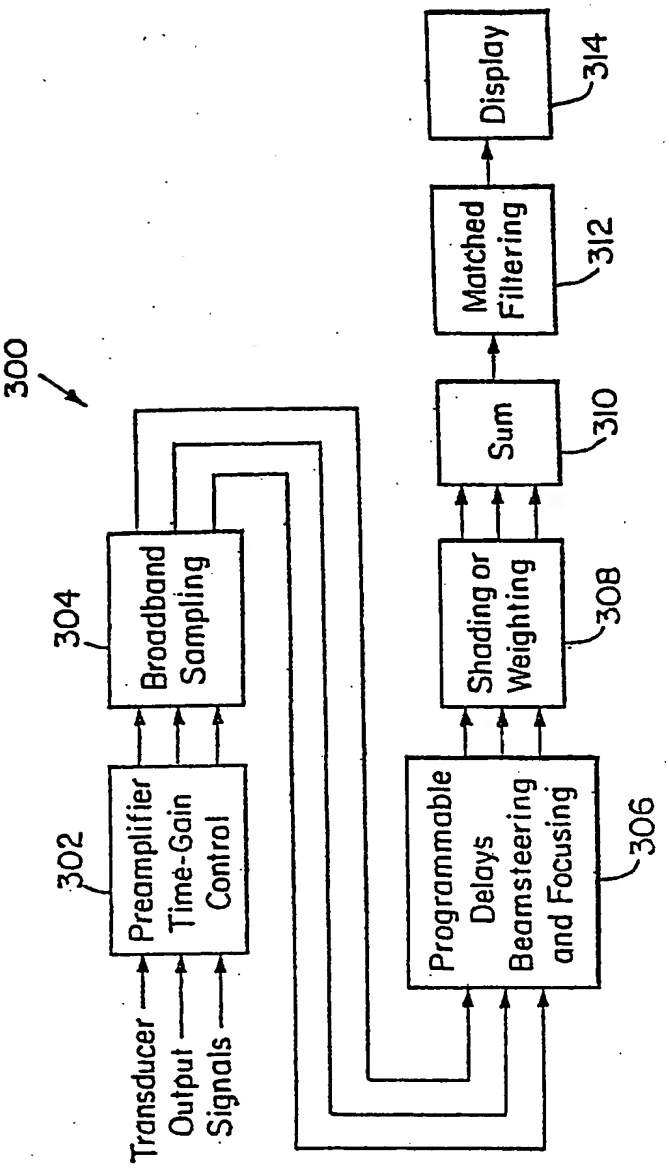
300
Display
314
Matched Filtering
312
Sum
310
Shading or Weighting
308
Programmable Delays Beamsteering and Focusing
306
Broadband Sampling
304
Preamplifier Time-Gain Control
302
Transducer Output Signals

FIG. 12

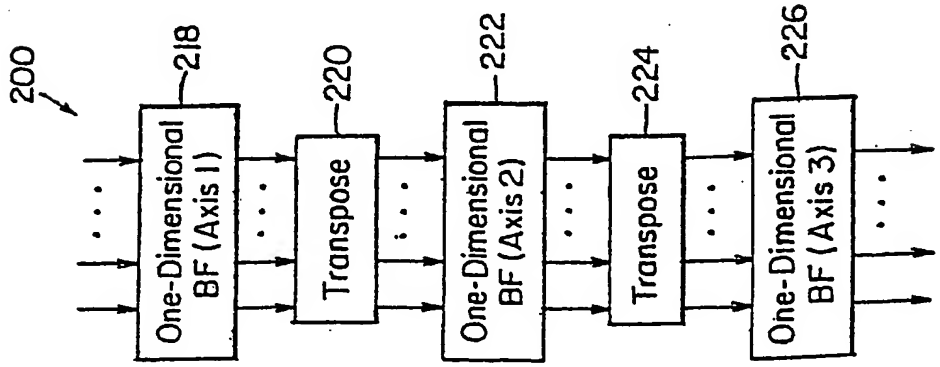
200
One-Dimensional BF (Axis 1)
218
Transpose
220
One-Dimensional BF (Axis 2)
222
Transpose
224
One-Dimensional BF (Axis 3)
226

FIG. 11

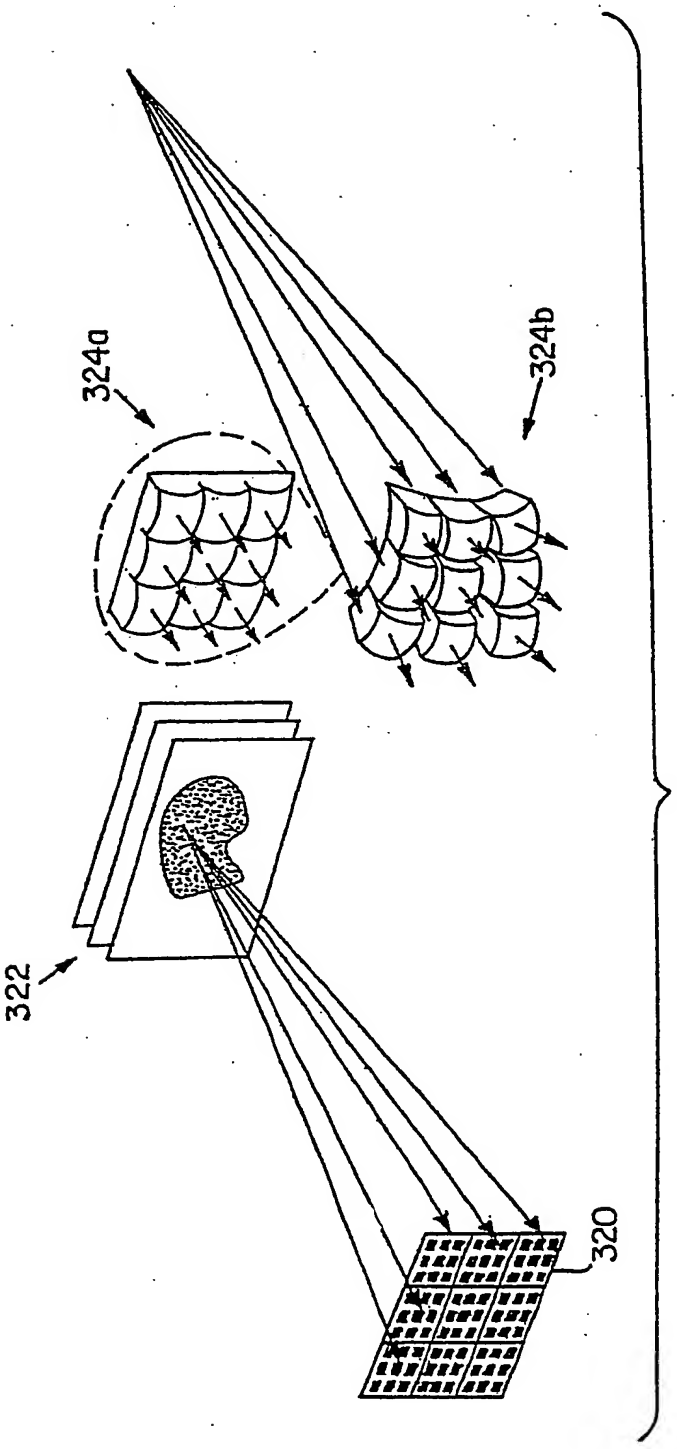

FIG. 13

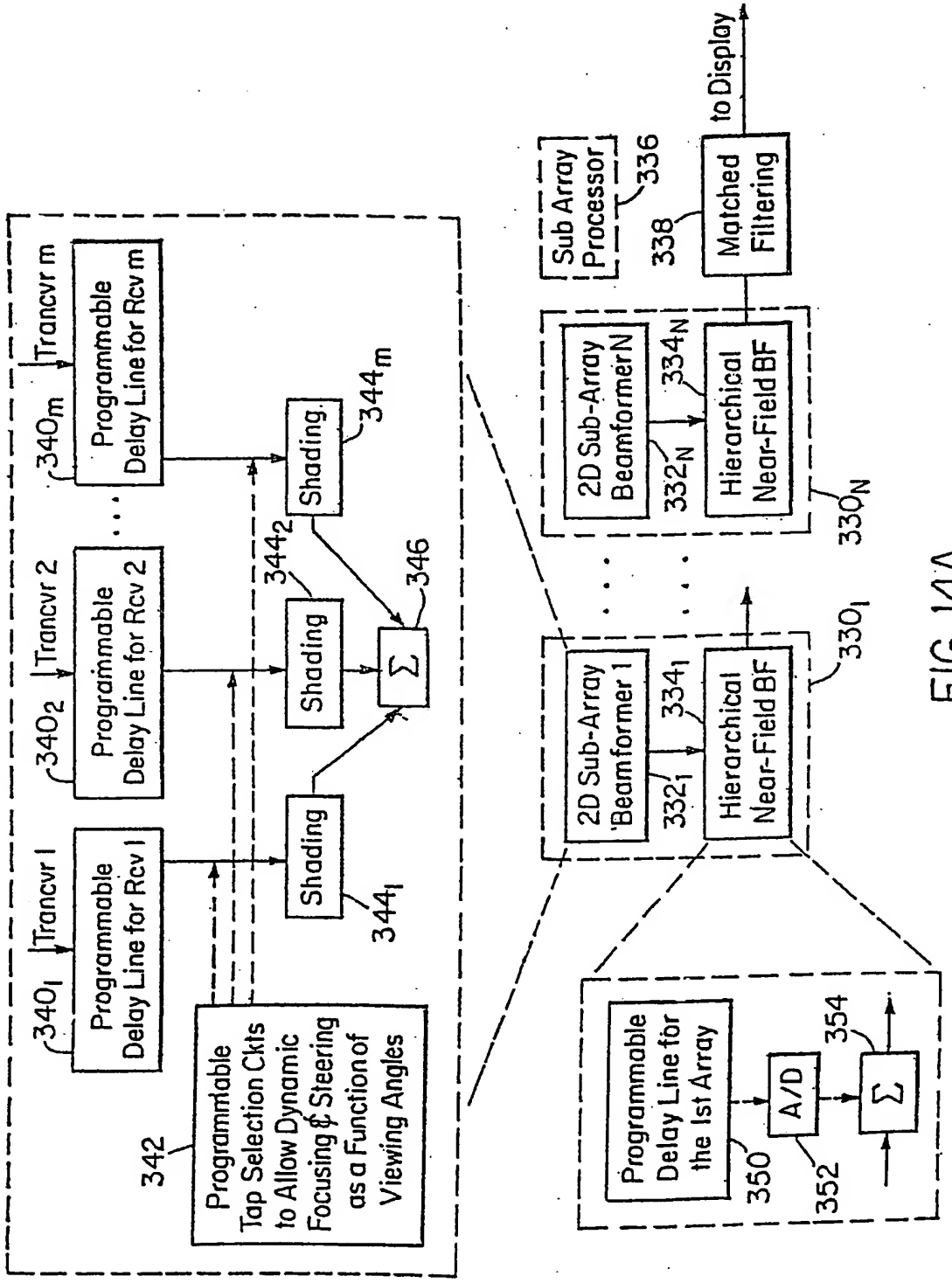
Trancvr 1
Trancvr 2
Trancvr m
Programmable Delay Line for Rcv 1
Programmable Delay Line for Rcv 2
Programmable Delay Line for Rcv m
340_1
340_2
340_m
Shading
344_1
344_2
344_m
346
342
Programmable Tap Selection Ckts to Allow Dynamic Focusing & Steering as a Function of Viewing Angles
2D Sub-Array Beamformer 1
2D Sub-Array BeamformerN
332_1
332_N
334_1
334_N
Hierarchical Near-Field BF
330_1
330_N
Sub Array Processor
336
338
Matched Filtering
to Display
Programmable Delay Line for the 1st Array
A/D
350
352
354

FIG. 14A

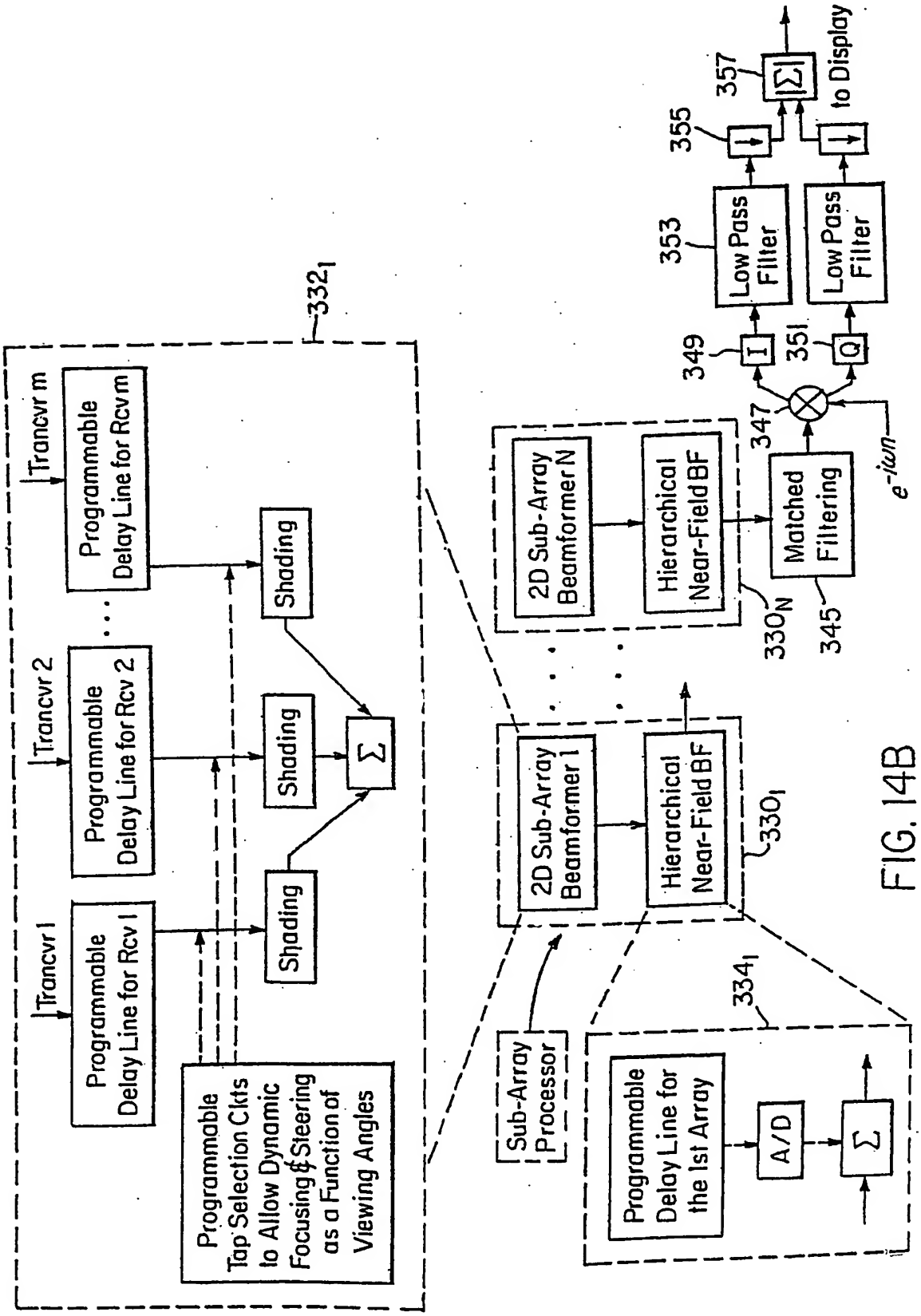
Trancvr 1
Trancvr 2
Trancvr m
Programmable Delay Line for Rcv 1
Programmable Delay Line for Rcv 2
Programmable Delay Line for Rcvm
Shading
Shading
Shading
Σ
Programmable Tap Selection Ckts to Allow Dynamic Focusing & Steering as a Function of Viewing Angles
332₁
Sub-Array Processor
2D Sub-Array Beamformer 1
Hierarchical Near-Field BF
330₁
2D Sub-Array Beamformer N
Hierarchical Near-Field BF
330N
Programmable Delay Line for the 1st Array
A/D
Σ
334₁
345
Matched Filtering
347
e^-iωn
349
I
351
Q
353
Low Pass Filter
Low Pass Filter
355
357
|Σ|
to Display

FIG. 14B

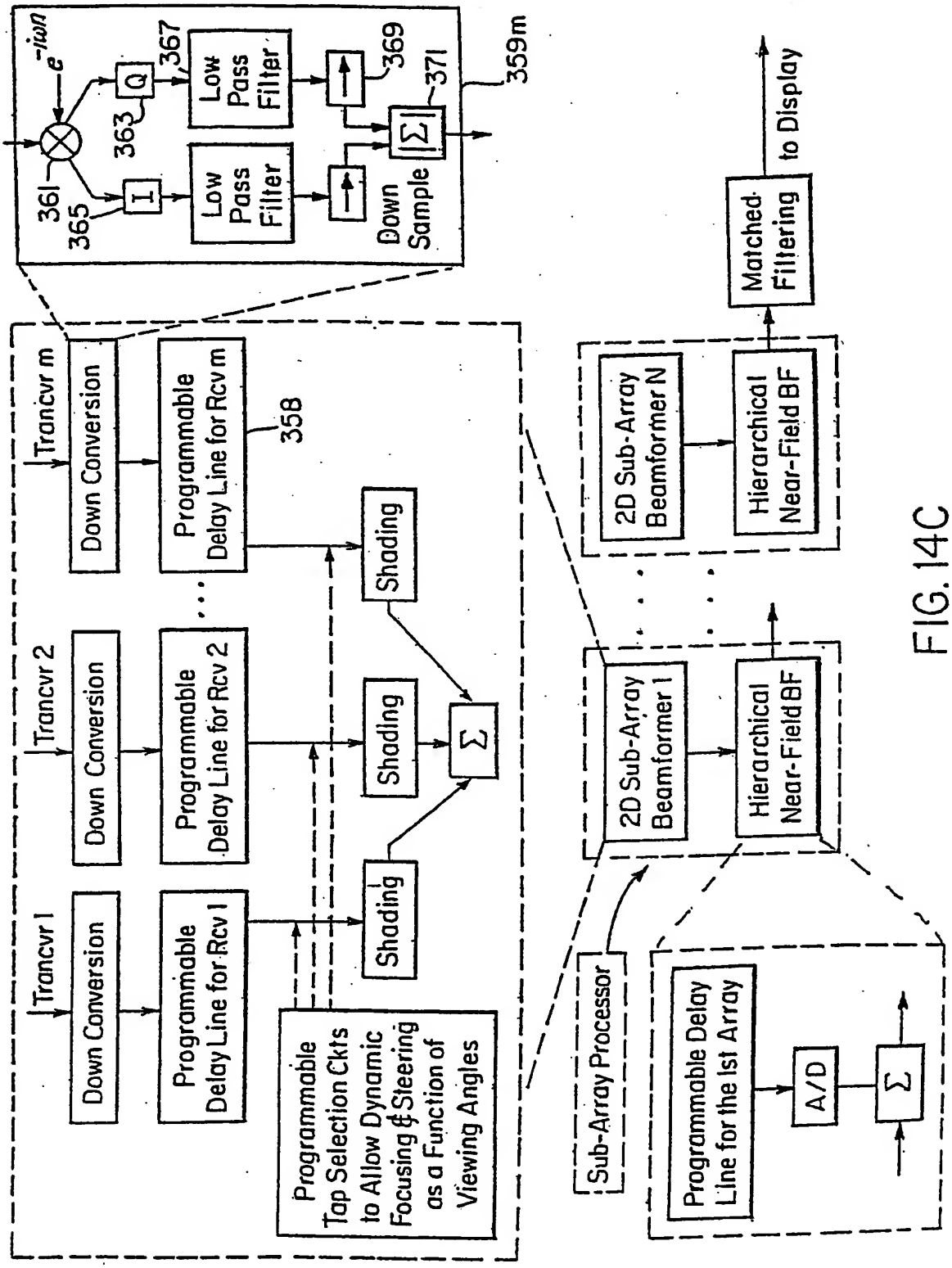
Trancvr 1
Trancvr 2
Trancvr m
Down Conversion
Programmable Delay Line for Rcv 1
Programmable Delay Line for Rcv 2
Programmable Delay Line for Rcv m
358
Shading
Programmable Tap Selection Ckts to Allow Dynamic Focusing & Steering as a Function of Viewing Angles
Σ
Sub-Array Processor
2D Sub-Array Beamformer 1
2D Sub-Array Beamformer N
Hierarchical Near-Field BF
Matched Filtering
to Display
Programmable Delay Line for the 1st Array
A/D
361
365
363
367
369
371
359m
I
Q
Low Pass Filter
Down Sample
$e^{-i\omega n}$

FIG. 14C

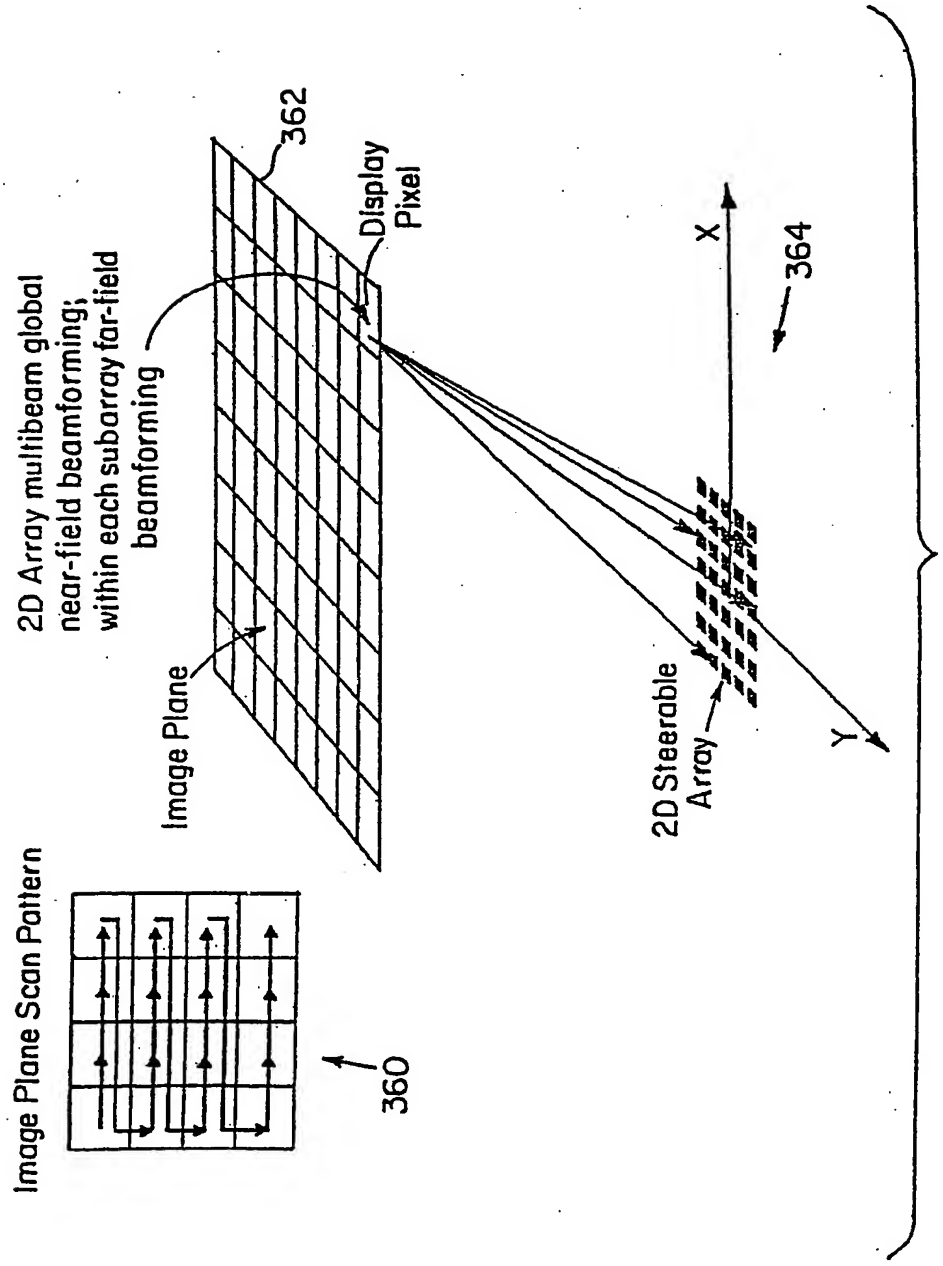
Image Plane Scan Pattern
360
Image Plane
2D Array multibeam global near-field beamforming; within each subarray far-field beamforming
362
Display Pixel
2D Steerable Array
X
Y
364

FIG. 15

FIG. 16

$$\hat{f}(x_0+1,y_0)=\hat{f}(x_0,y_0)+\Delta|_x^1 \hat{f}(x_0,y_0)$$

$$\hat{f}(x_0,y_0+1)=\hat{f}(x_0,y_0)+\Delta|_y^1 \hat{f}(x_0,y_0)$$

$$\hat{f}(x_0+1,y_0)\,\hat{f}(x_0,y_0+1)=$$

$$\hat{f}(x_0+1,y_0)\,\hat{f}(x_0,y_0)+\hat{f}(x_0,y_0+1)\,\hat{f}(x_0,y_0+\Delta|_x^1\Delta|_y^1\hat{f}(x_0,y_0)-\hat{f}(x_0,y_0)\,\hat{f}(x_0,y_0)$$

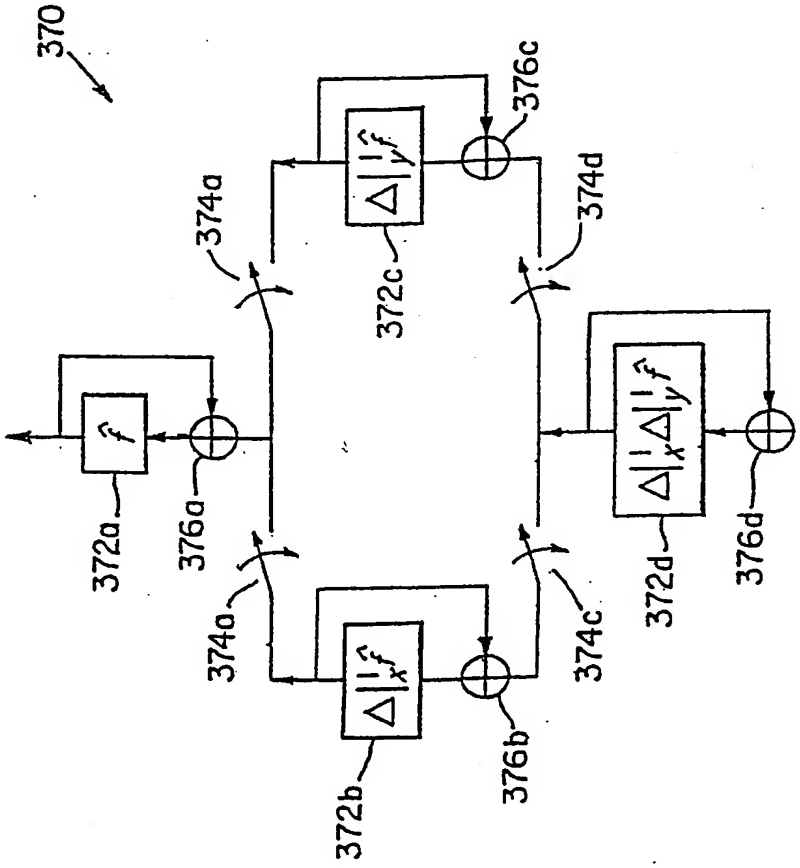

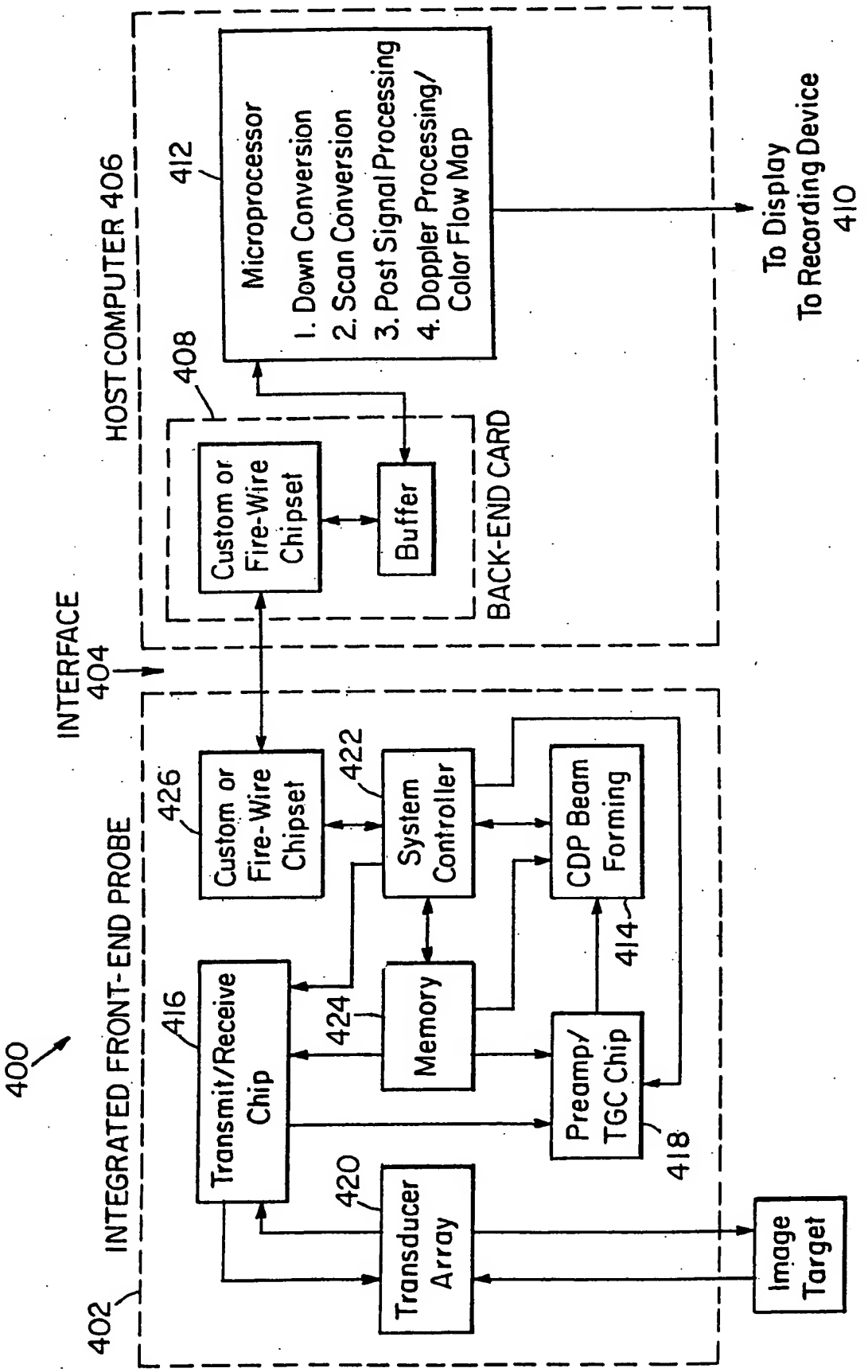
400
INTEGRATED FRONT-END PROBE
402
INTERFACE
404
HOST COMPUTER 406
BACK-END CARD
408
Microprocessor
412
1. Down Conversion
2. Scan Conversion
3. Post Signal Processing
4. Doppler Processing/ Color Flow Map
Custom or Fire-Wire Chipset
Buffer
To Display
To Recording Device
410
Custom or Fire-Wire Chipset
426
System Controller
422
CDP Beam Forming
414
Transmit/Receive Chip
416
Memory
424
Preamp/ TGC Chip
418
Transducer Array
420
Image Target

FIG. 17A

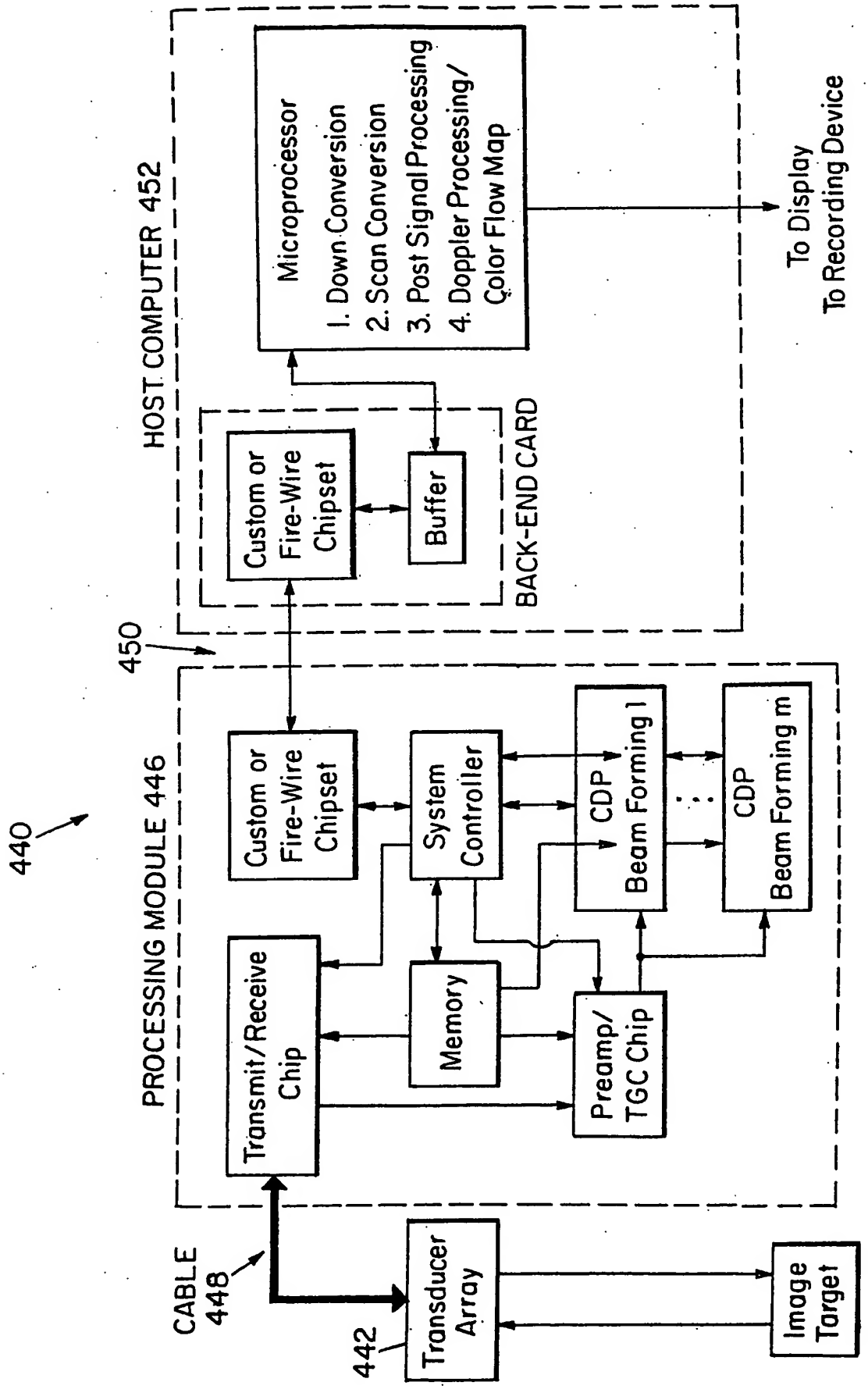
440
HOST COMPUTER 452
Microprocessor
1. Down Conversion
2. Scan Conversion
3. Post Signal Processing
4. Doppler Processing/
Color Flow Map
To Display
To Recording Device
BACK-END CARD
Custom or
Fire-Wire
Chipset
Buffer
450
PROCESSING MODULE 446
Custom or
Fire-Wire
Chipset
System
Controller
CDP
Beam Forming 1
CDP
Beam Forming m
Transmit/Receive
Chip
Memory
Preamp/
TGC Chip
CABLE
448
442
Transducer
Array
Image
Target

FIG. 17B

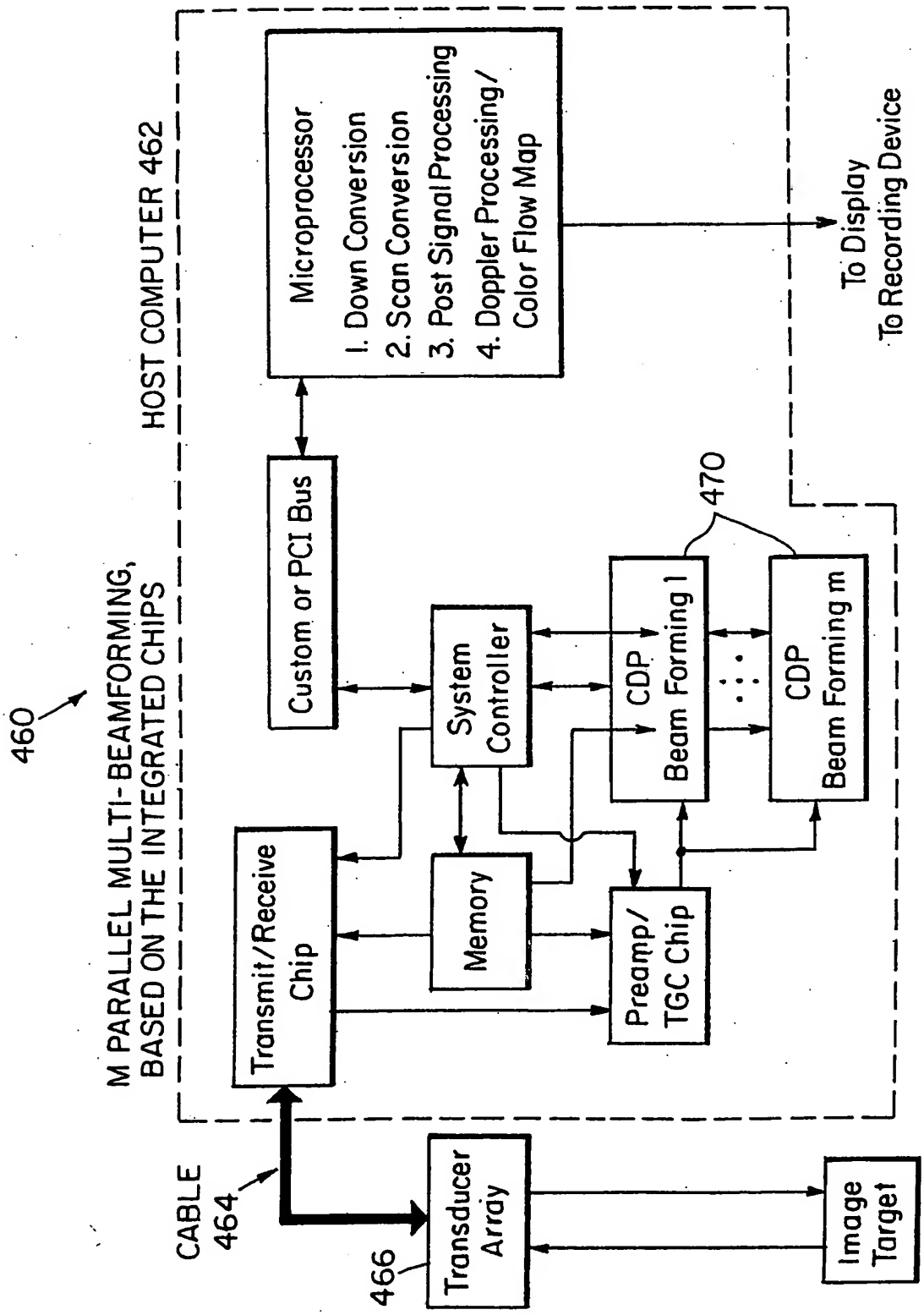
460
M PARALLEL MULTI-BEAMFORMING, BASED ON THE INTEGRATED CHIPS
HOST COMPUTER 462
Microprocessor
1. Down Conversion
2. Scan Conversion
3. Post Signal Processing
4. Doppler Processing/ Color Flow Map
To Display
To Recording Device
Custom or PCI Bus
System Controller
470
CDP Beam Forming 1
CDP Beam Forming m
Transmit/Receive Chip
Memory
Preamp/ TGC Chip
CABLE 464
466
Transducer Array
Image Target

FIG. 17C

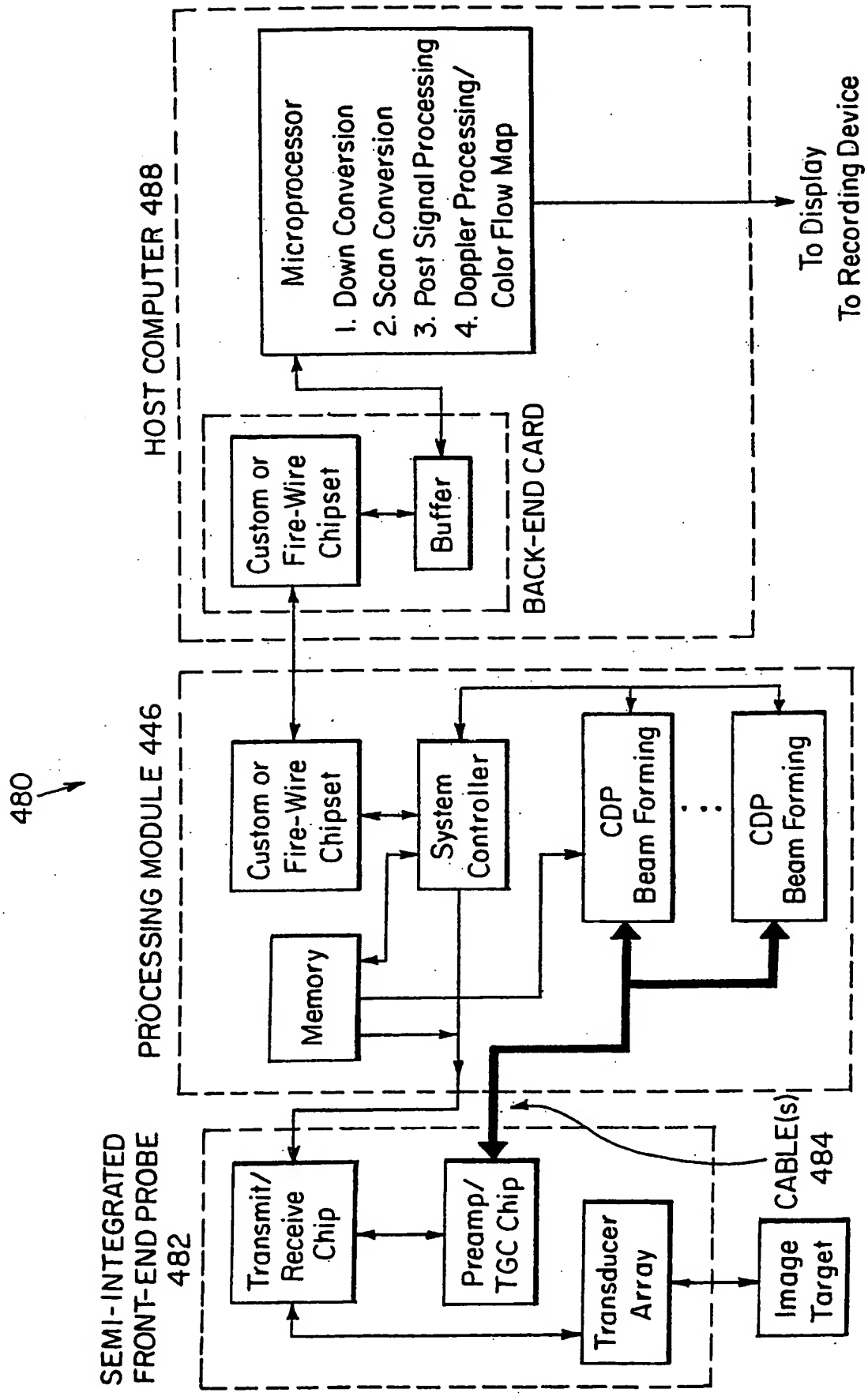
480
HOST COMPUTER 488
Microprocessor
1. Down Conversion
2. Scan Conversion
3. Post Signal Processing
4. Doppler Processing/
Color Flow Map
To Display
To Recording Device
BACK-END CARD
Custom or
Fire-Wire
Chipset
Buffer
PROCESSING MODULE 446
Custom or
Fire-Wire
Chipset
System
Controller
CDP
Beam Forming
CDP
Beam Forming
Memory
SEMI-INTEGRATED
FRONT-END PROBE
482
Transmit/
Receive
Chip
Preamp/
TGC Chip
Transducer
Array
Image
Target
CABLE(s)
484

FIG. 17D

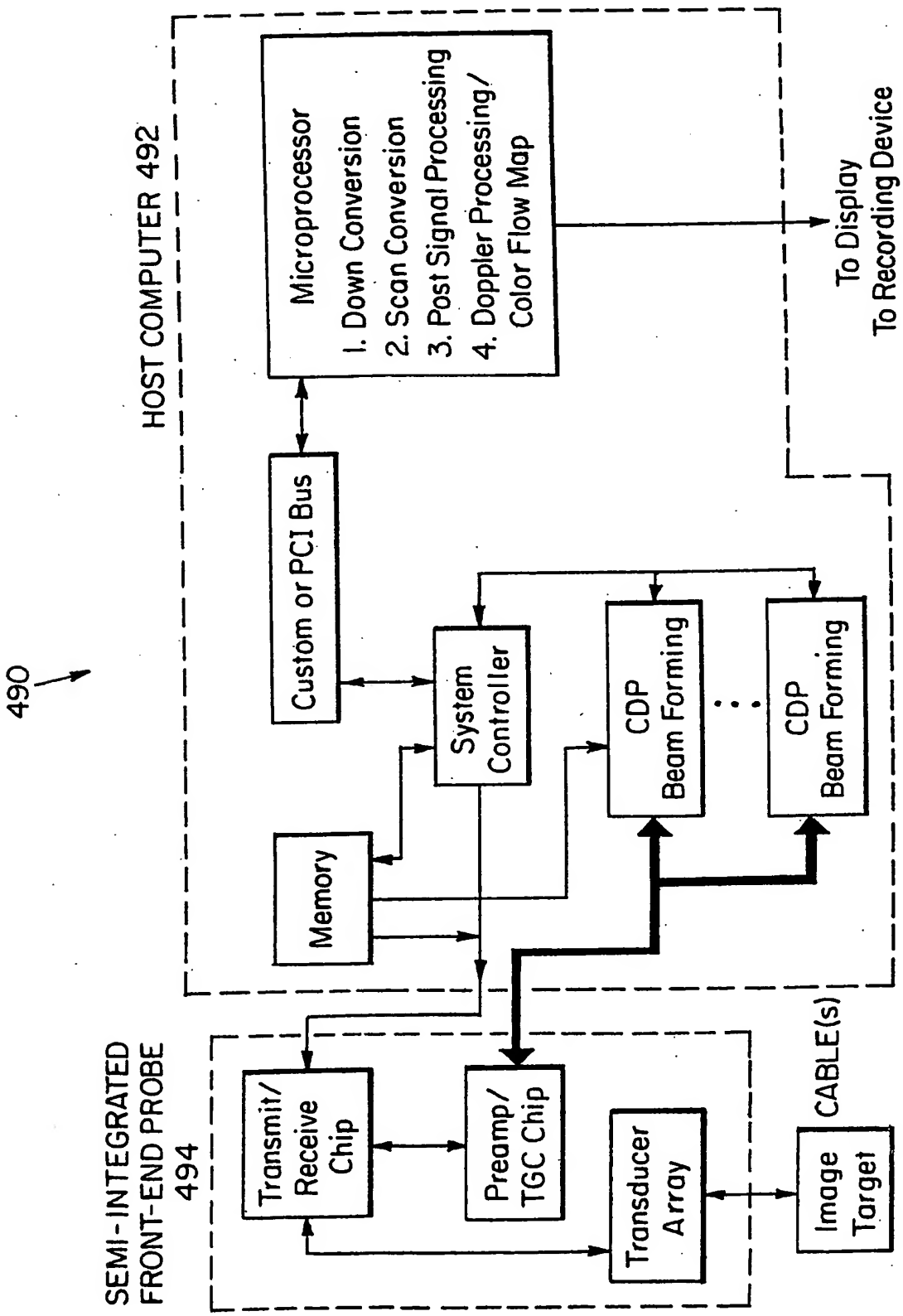
490
HOST COMPUTER 492
Microprocessor
1. Down Conversion
2. Scan Conversion
3. Post Signal Processing
4. Doppler Processing/
Color Flow Map
To Display
To Recording Device
Custom or PCI Bus
System Controller
CDP Beam Forming
CDP Beam Forming
Memory
SEMI-INTEGRATED FRONT-END PROBE 494
Transmit/ Receive Chip
Preamp/ TGC Chip
Transducer Array
CABLE(s)
Image Target

FIG. 17E

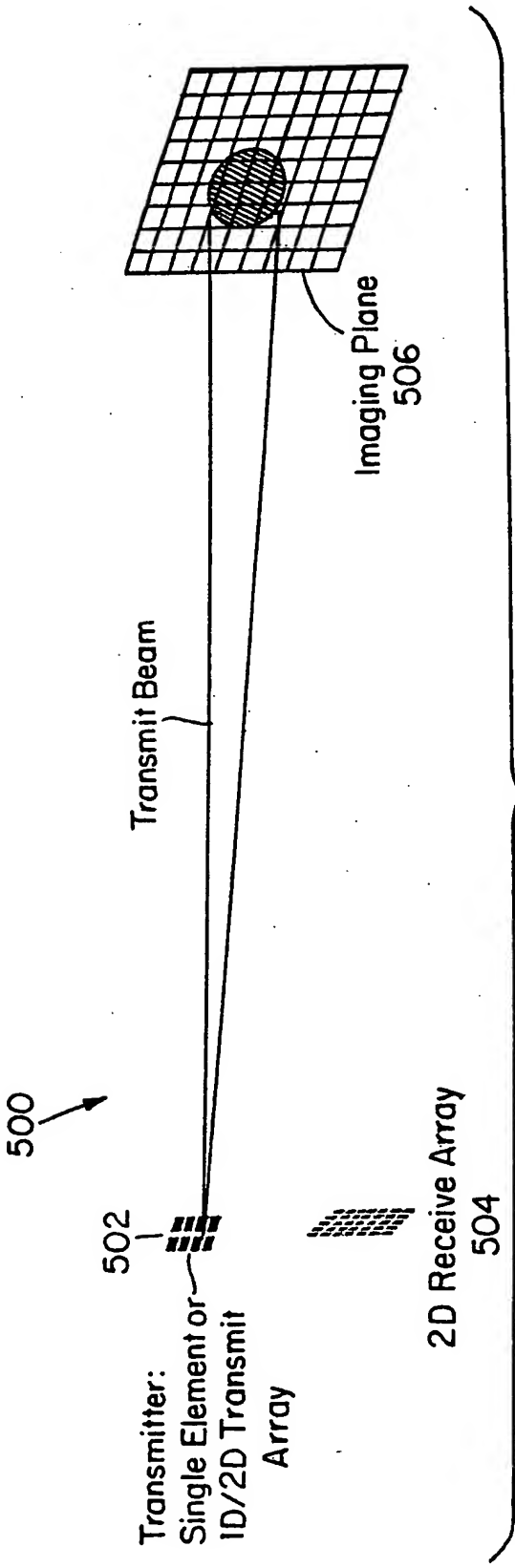

FIG. 18A

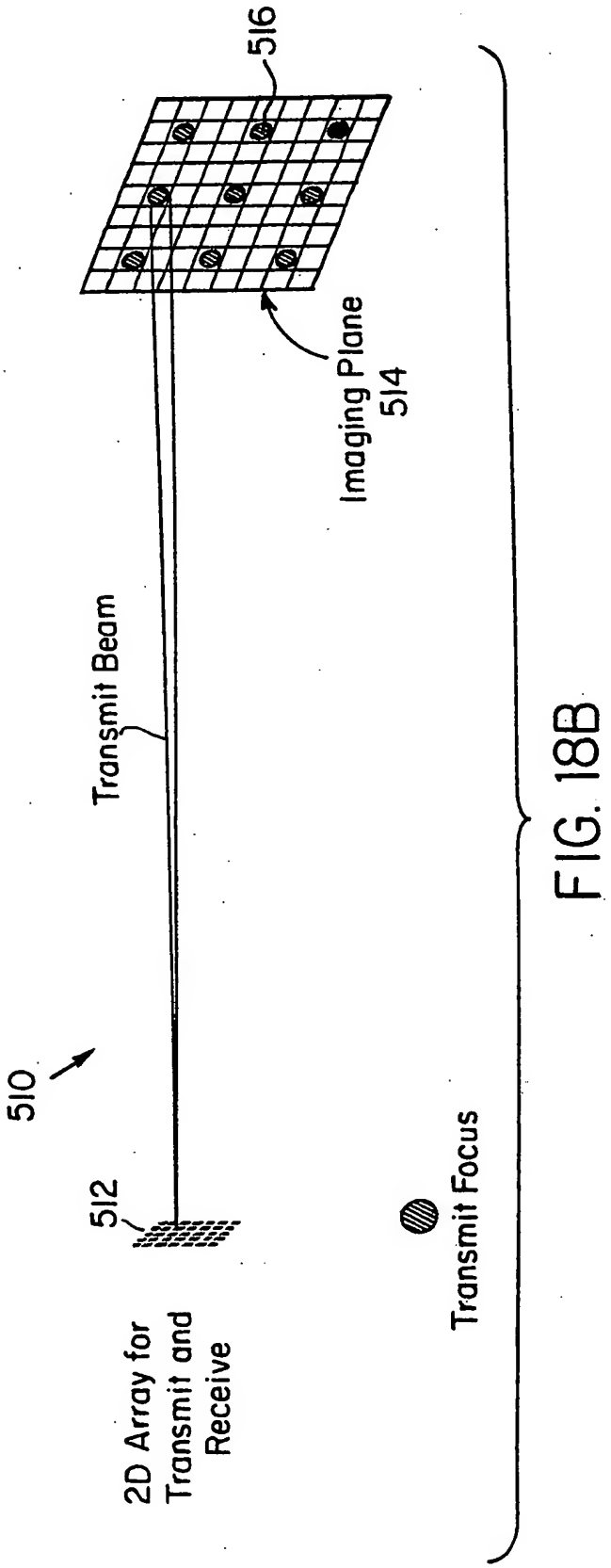

FIG. 18B

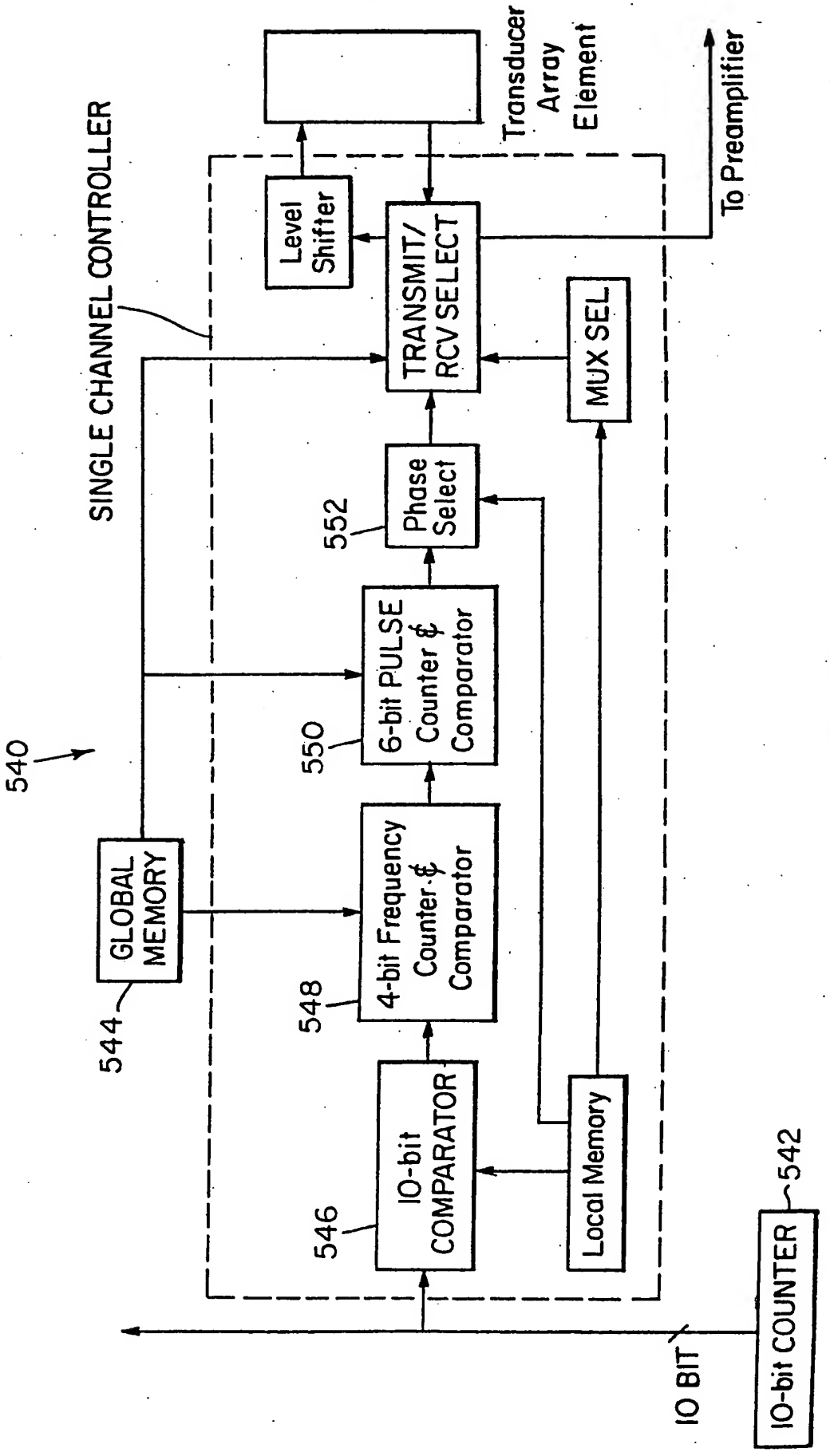
SINGLE CHANNEL CONTROLLER
540
Transducer Array Element
To Preamplifier
Level Shifter
TRANSMIT/ RCV SELECT
MUX SEL
552
Phase Select
550
6-bit PULSE Counter & Comparator
544
GLOBAL MEMORY
548
4-bit Frequency Counter & Comparator
546
10-bit COMPARATOR
Local Memory
542
10-bit COUNTER
10 BIT

FIG. 19

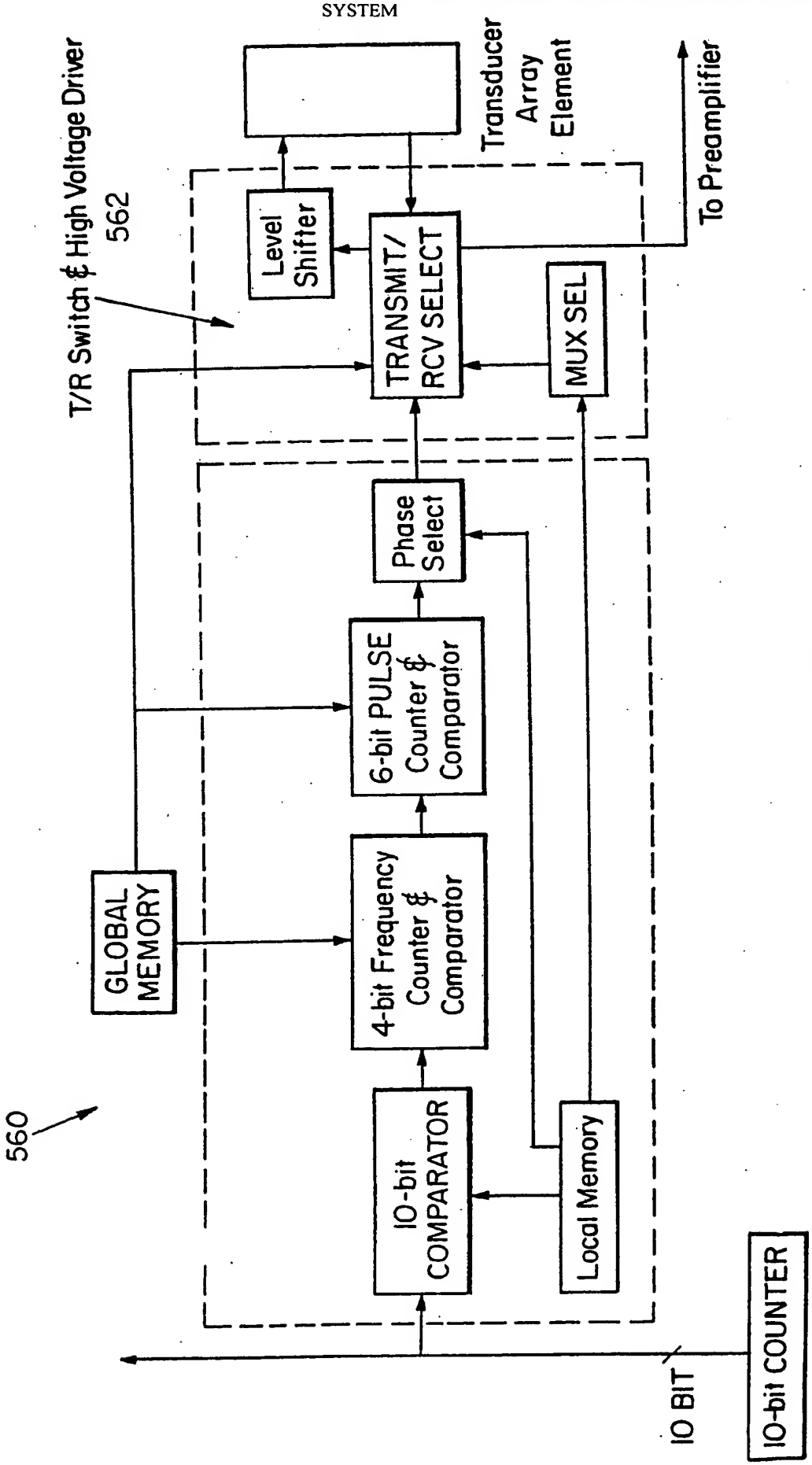
560
T/R Switch & High Voltage Driver
562
Transducer Array Element
To Preamplifier
Level Shifter
TRANSMIT/ RCV SELECT
MUX SEL
Phase Select
6-bit PULSE Counter & Comparator
4-bit Frequency Counter & Comparator
GLOBAL MEMORY
10-bit COMPARATOR
Local Memory
10 BIT
10-bit COUNTER

FIG. 20

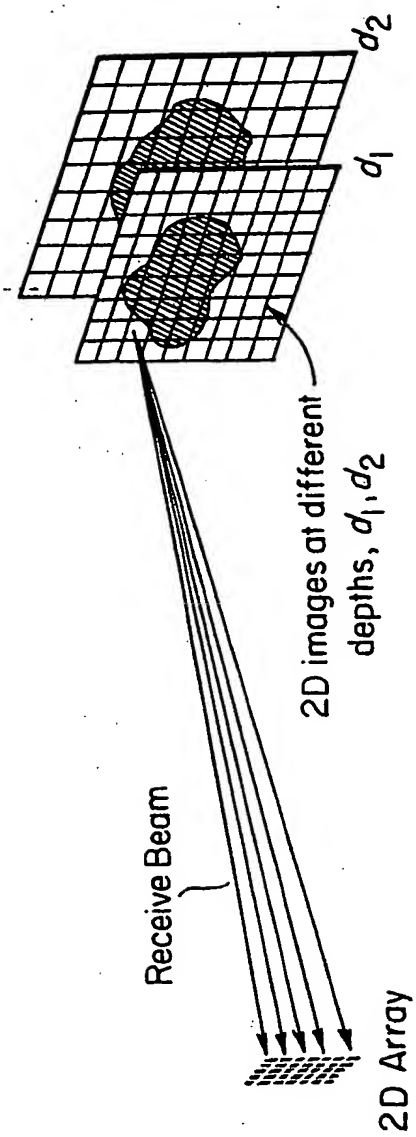

FIG. 21A

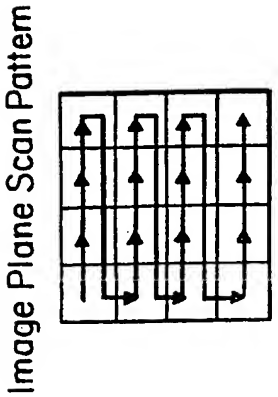

FIG. 21B

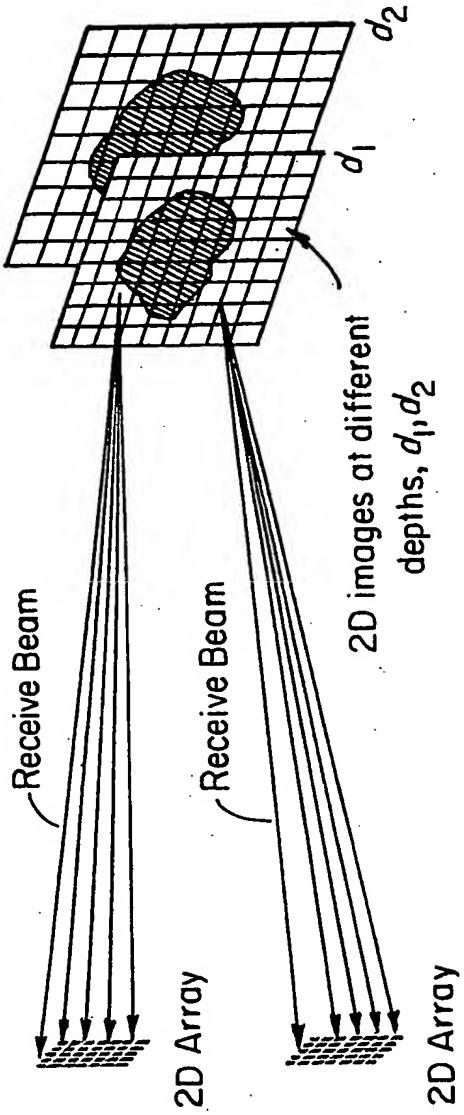

FIG. 21C

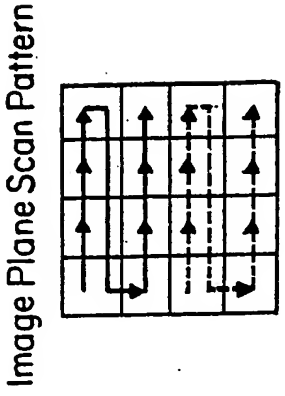

FIG. 21D

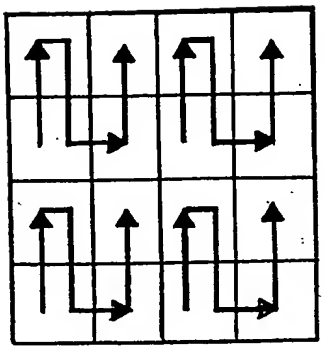

Four-Processor System

FIG. 22C

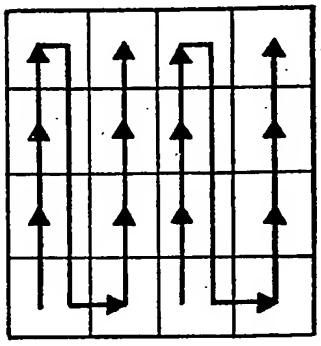

Two-Processor System

FIG. 22B

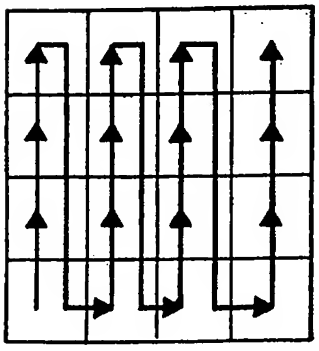

Single-Processor System

FIG. 22A

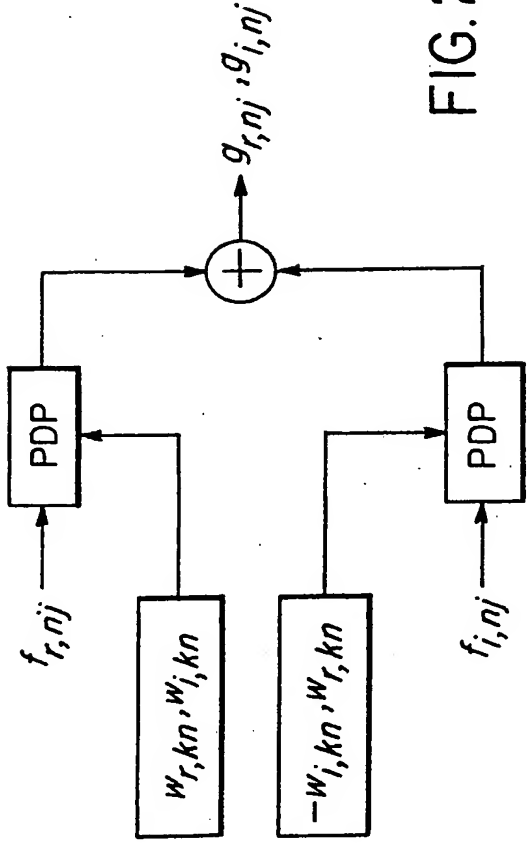

FIG. 27

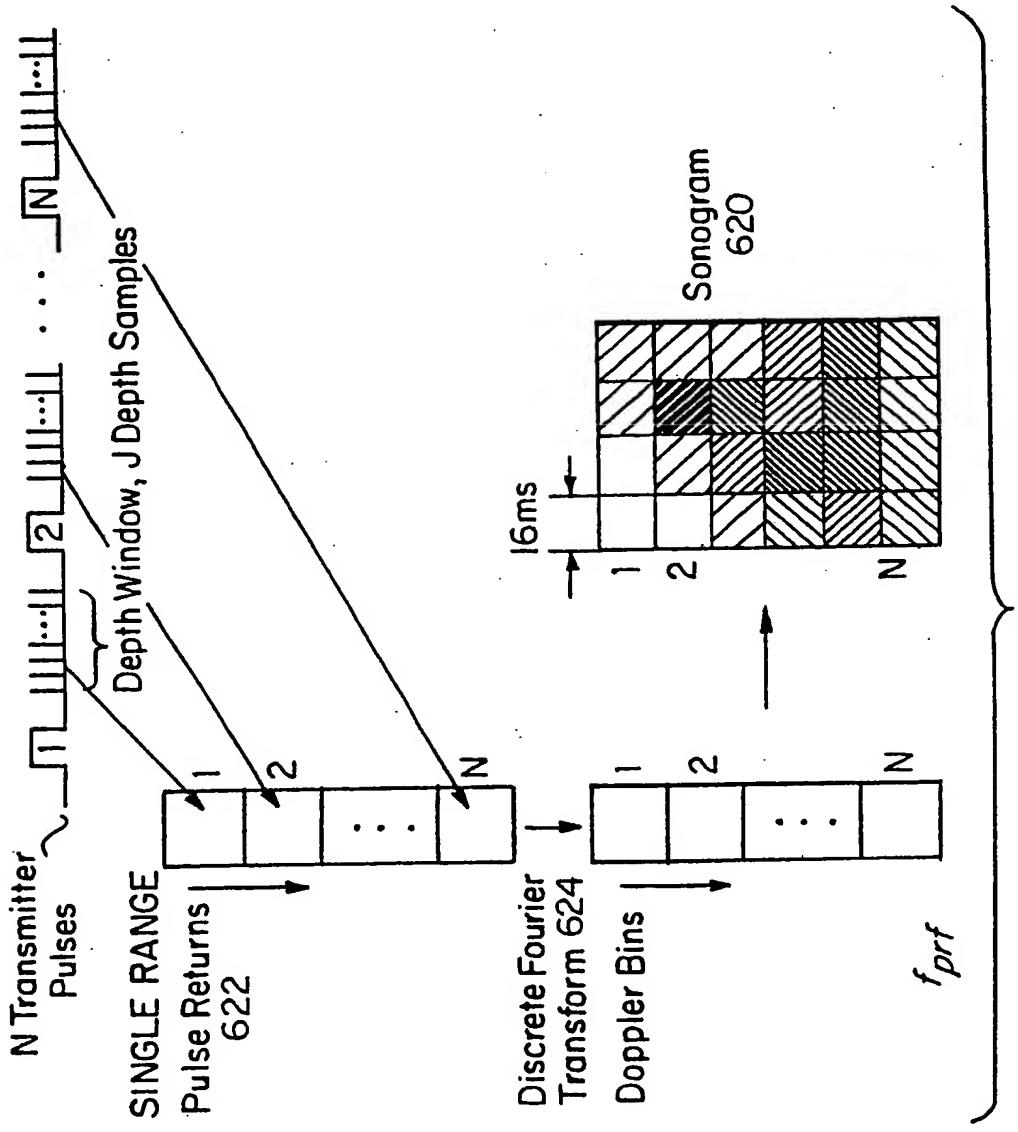
N Transmitter Pulses
1
2
N
Depth Window, J Depth Samples
SINGLE RANGE
Pulse Returns
622
Discrete Fourier Transform 624
Doppler Bins
Sonogram
620
16ms
f_{prf}

FIG. 24

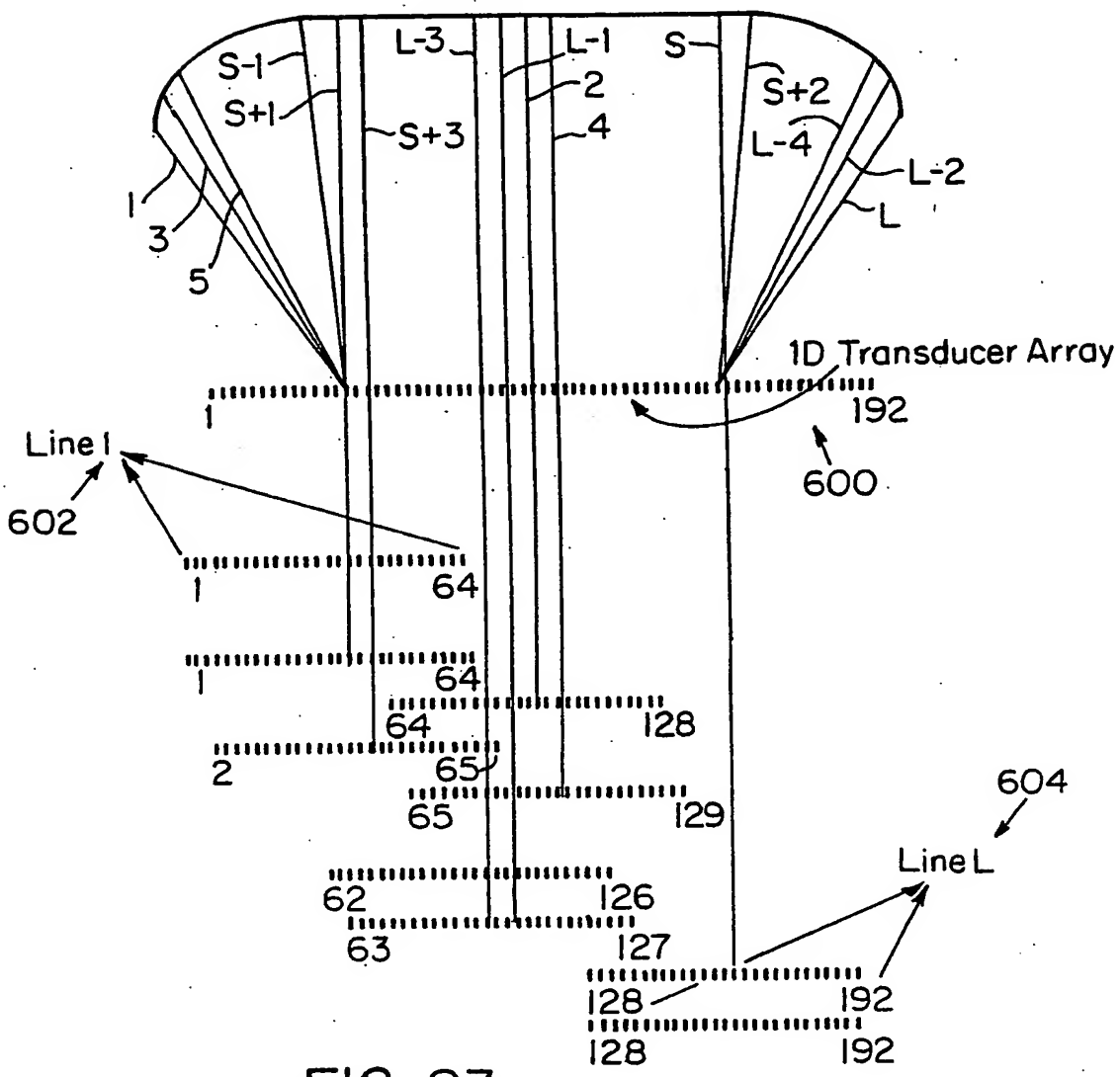

FIG. 23

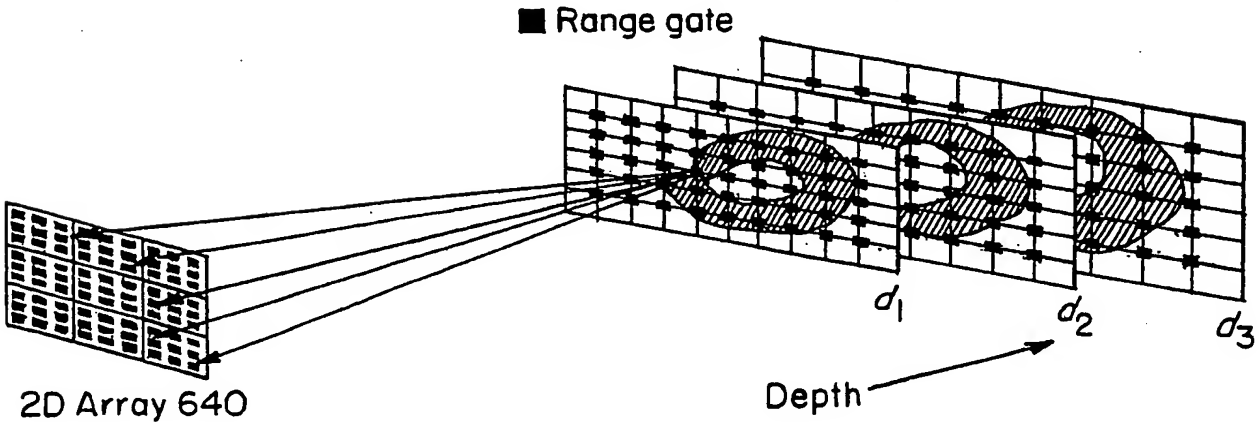

FIG. 25

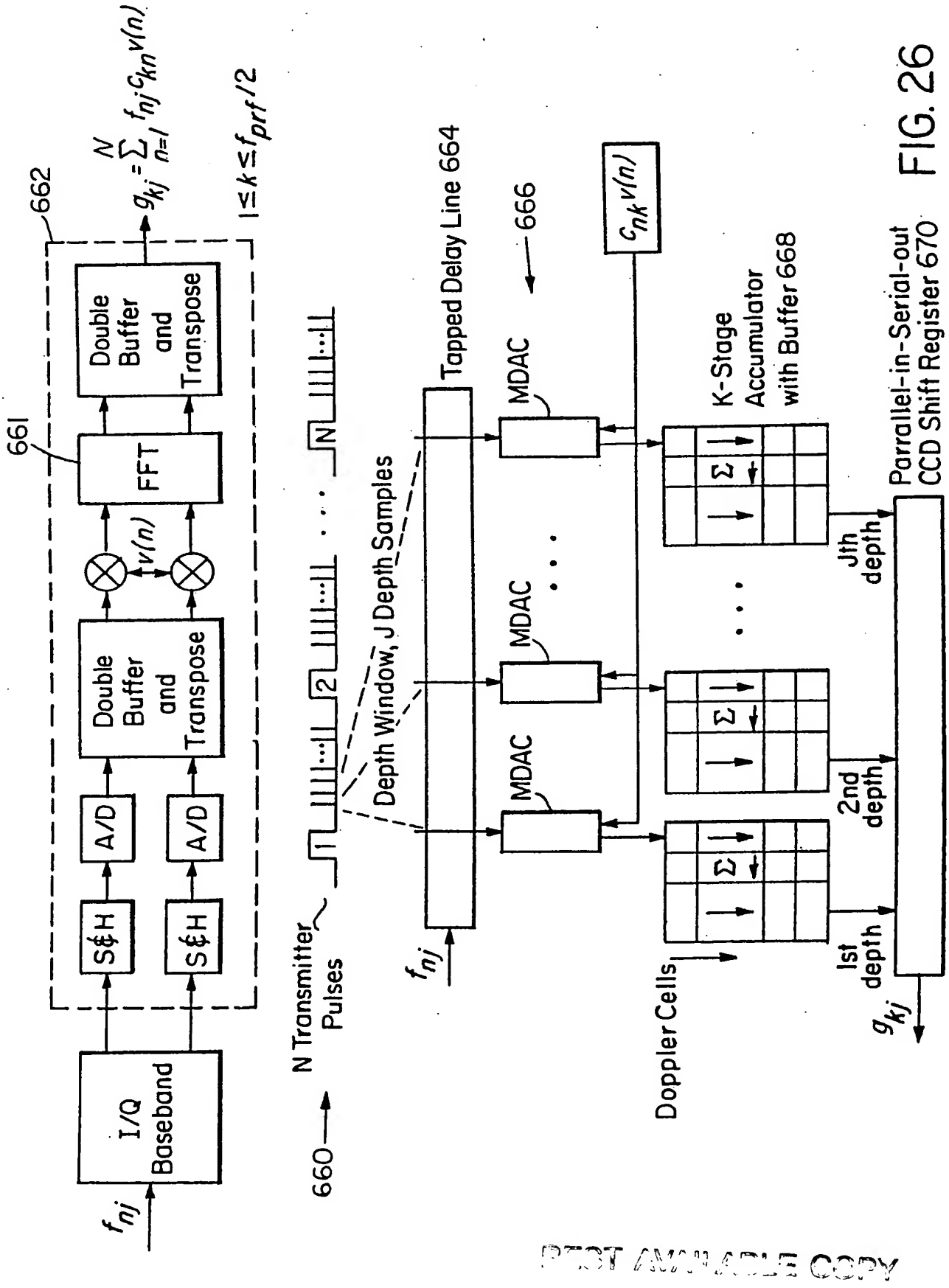

FIG. 26

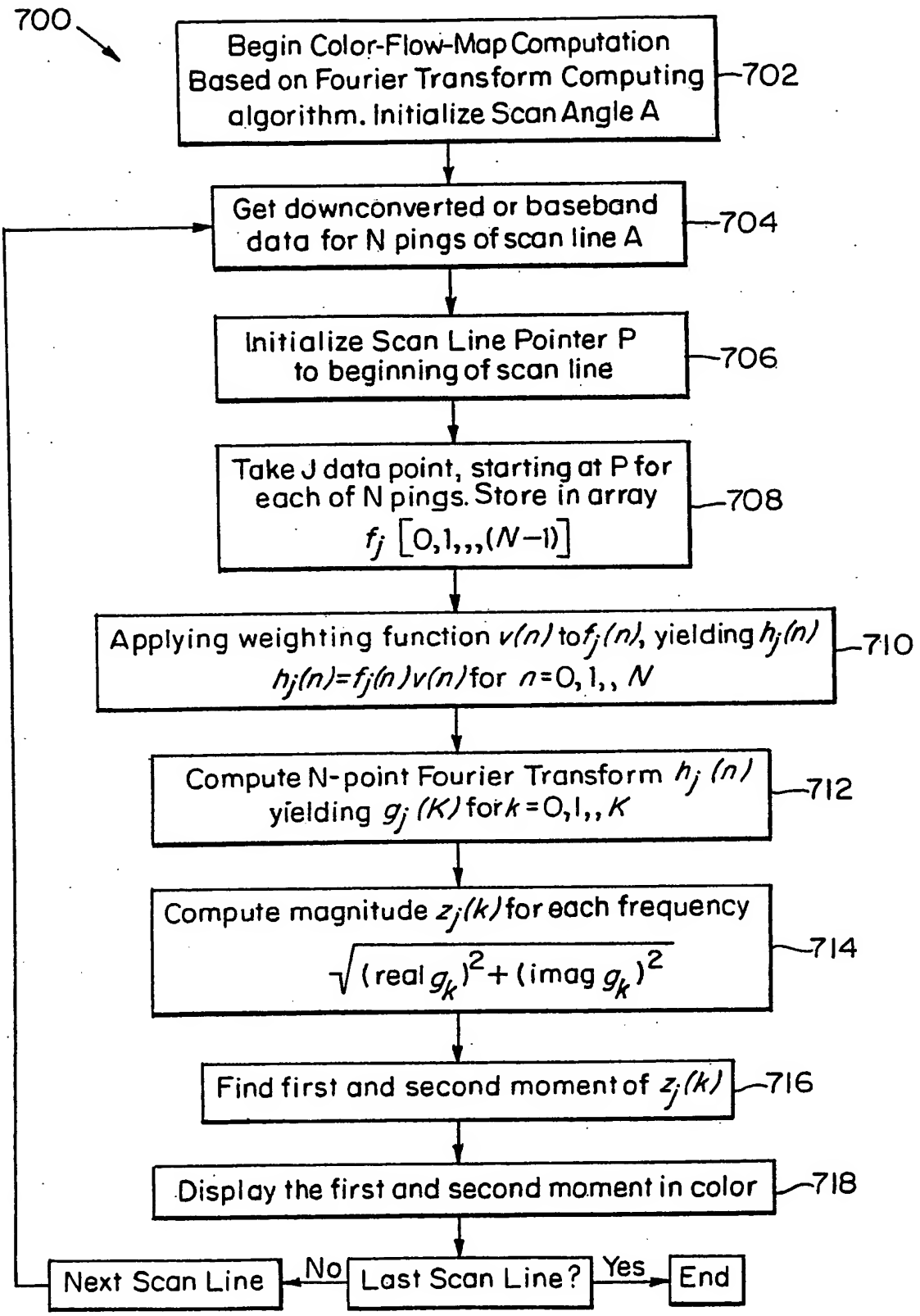

FIG. 28

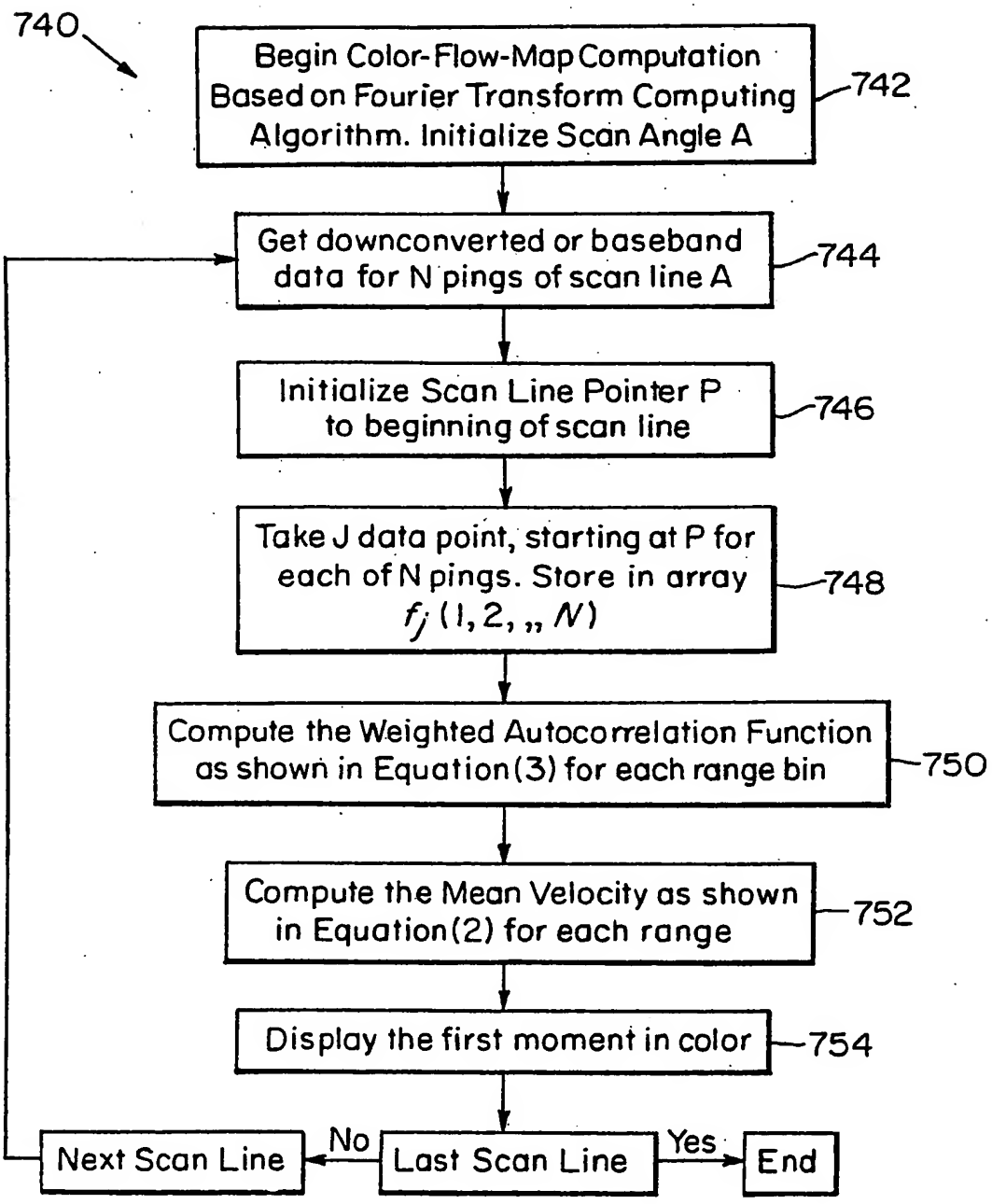

FIG. 29

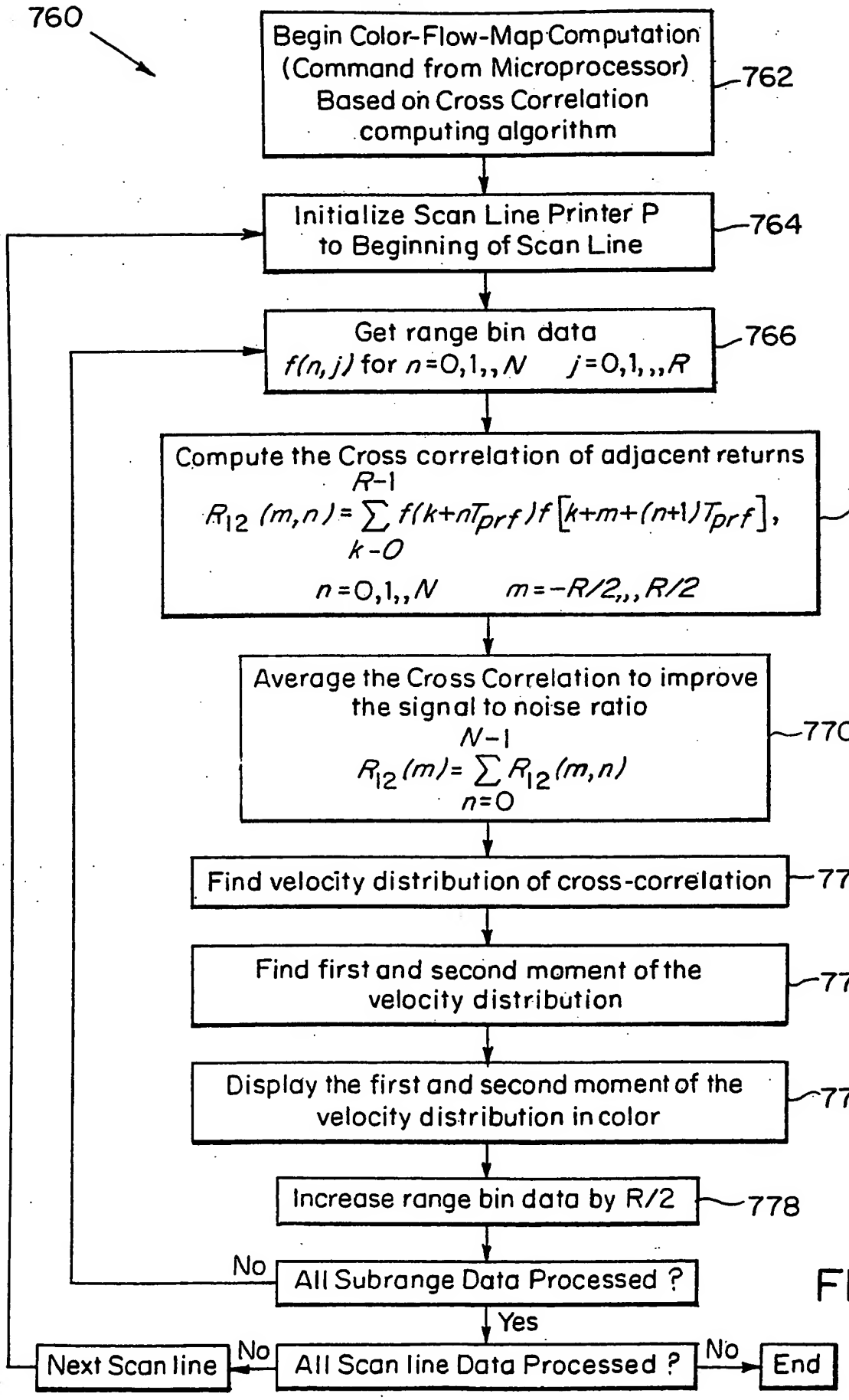
760
Begin Color-Flow-Map Computation (Command from Microprocessor) Based on Cross Correlation computing algorithm
762
Initialize Scan Line Printer P to Beginning of Scan Line
764
Get range bin data
f(n,j) for n=0,1,,N j=0,1,,,R
766
Compute the Cross correlation of adjacent returns
$R_{12}(m,n) = \sum_{k-0}^{R-1} f(k+nT_{prf}) f[k+m+(n+1)T_{prf}]$,
n=0,1,,N m=-R/2,,,R/2
768
Average the Cross Correlation to improve the signal to noise ratio
$R_{12}(m) = \sum_{n=0}^{N-1} R_{12}(m,n)$
770
Find velocity distribution of cross-correlation
772
Find first and second moment of the velocity distribution
774
Display the first and second moment of the velocity distribution in color
776
Increase range bin data by R/2
778
No
All Subrange Data Processed ?
Yes
Next Scan line
No
All Scan line Data Processed ?
No
End

FIG. 30